Master's Thesis

Design and optimization of cell components for liquid metal battery and investigation of low operating temperature molten salt electrolyte with Li|LiCl-LiI-KI|Bi composition

YoungJae Jung

Department of Energy Engineering

(Battery Science and Technology)

Graduate School of UNIST

2019

Design and optimization of cell components for liquid metal battery and investigation of low operating temperature molten salt electrolyte with with Li|LiCl-LiI-KI|Bi composition

YoungJae Jung

Department of Energy Engineering
(Battery Science and Technology)

Graduate School of UNIST

Design and optimization of cell components for liquid metal battery and investigation of low operating temperature molten salt electrolyte with Li|LiCl-LiI-KI|Bi composition

A thesis/dissertation
submitted to the Graduate School of UNIST
in partial fulfillment of the
requirements for the degree of
Master of Science

YoungJae Jung

01/08/2019

Approved by

Advisor

Youngsik Kim

Design and optimization of cell components for liquid metal battery and investigation of low operating temperature molten salt electrolyte with Li|LiCl-LiI-KI|Bi composition

YoungJae Jung

This certifies that the thesis/dissertation of YoungJae Jung is approved.

01/08/2019

signature

Advisor: Youngsik Kim

signature

Yunseok Choi: Thesis Committee Member #1

signature

Seok Ju Kang: Thesis Committee Member #2

Abstract

Liquid metal batteries (LMBs) are good candidate for mass energy storage system due to their high rate capability and long cycle life. However, most metal electrodes have high melting point and this high temperature can cause thermal corrosion and maintenance cost problem. To reduce the operating temperature, many electrode compositions were tested such as Mg||Sb, Li||Sb, Li||Sb-Pb but there was no test related with electrolytes yet. Here, we focus on the molten salt electrolyte, and its properties, melting temperature, ionic conductivity, solubility and so on.

Before test on the change of active materials, the optimization of cell test condition such as sealing method and cell design must be established. Therefore, we set up 2 factors which affect the cell performance, i) repeatability factor and ii) unstable cell voltage factor and tested cell at various condition to make reference data for each factor.

The previous lowest operating temperature of Lithium based LMB is 410 ℃, using Li|LiCl-LiI|Bi composition. The melting points of Li metal and Bi metal are 180 ℃ and 270 ℃, respectively. However, the melting temperature of LiCl-LiI molten salt electrolyte is 370 ℃. To reduce the melting temperature of molten salt, we added KI (potassium iodide) to LiCl-LiI molten salt and made LiCl-LiI-KI salt (265 ℃, eutectic). Consequently, we can reduce the operating temperature to 300 ℃ which is verified through differential scanning calorimetry and electrochemical impedance spectroscopy. Through Li|LiCl-LiI-KI|Bi composition, we tested cell operating performance at various temperature. While decreasing the temperature (400 ℃→300 ℃), the energy efficiency decrease (85.1% → 81.9%) because of decreased ionic conductivity of electrolyte at current density of 50 mA/cm². However, lowering temperature also increase the cell open circuit voltage because Li solubility in Bi metal decreased. The cell performance is also analyzed as post mortem by phase diagram and scanning electron microscopy and x-ray diffraction analysis.

Contents

List of figures

List of Tables

1. Introduction

1.1. Energy Storage System (ESS)

1.1.1 Needs for ESS

Nowadays the electrical grid system expects the electric power demand and generates the electricity from power plant correspondingly. Due to the supply is computed based on expected demand, the equilibrium of demand and supply is always inconsistent; the supplies are always larger than the demands to fulfill our needs constantly. We called these additional supplies as reserve margin, which is calculated by (capacity minus demand)/demand, where "capacity" is the expected maximum available supply and "demand" is expected peak demand[1]. In the republic of Korea, the reserve margin is about 20 ~ 40 % for every time and the amount is nearly 15 MW ~ 25MW according to time difference[2].

Figure 1. shows the daily power supply and demand in republic of Korea at September 28th, 2018. During the peak time, supply availability power capacity was 87.8 MW and current load demand was 64.7 MW so calculated reserve margin was 32% and these data are computed by Korea Power Exchange. These amounts of reserve electricity are unable to be stored so that the excess supply of energy is wasted every time. Therefore, if we can store energy, we can save large amount of energy. Also, energy storage can be utilized in many applications for integration of renewable energy and so on.

1.1.2 Functions of ESS

1.1.2.1 ESS for peak shaving

The main function of the energy storage system is reducing the peak demand of electrical grid. According to the Korea Electric Power Corporator, as shown in table 1, the electric rates at peak time is 2~3 times expensive than off-peak load time. Therefore, during the night and morning, when the price of the electricity is relatively inexpensive, generate the electricity and store the energy. During peak-time when the price of the electricity is expensive, use the stored electricity. This concept is 'peak shaving', reducing the peak demand as shown in figure 1; energy storage with high efficiency power plant, low energy cost during off-peak (red region) and use the energy during expensive energy cost peak-time (green region).

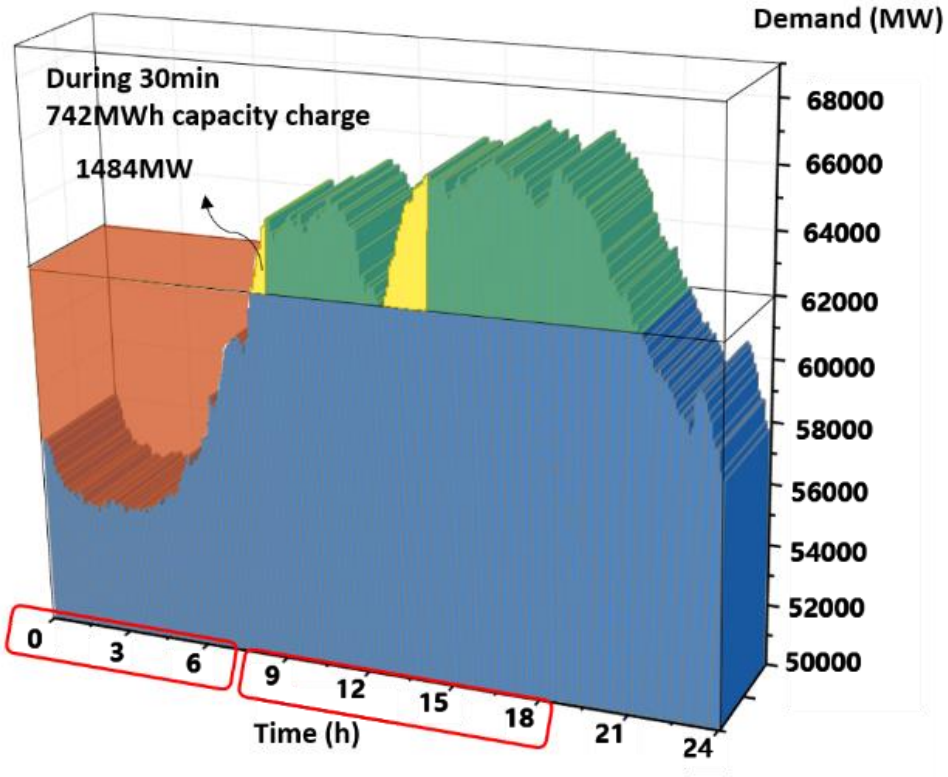

Figure 1. Electric energy demand in Korea at 2018.09.28

Classification		Demand Charge (won/kW)	Energy charge (won/kWh)			
			Time period	Summer (Jun~Aug)	Spring/fall (Mar~May) (Sep~Oct)	Winter (Nov~Feb)
High-Voltage A	Option I	7,220	Off-peak	61.6	61.6	68.6
			Mid-load	114.5	84.1	114.7
			Peak-load	196.6	114.8	172.2
	Option II	8,320	Off-peak	56.1	56.1	63.1
			Mid-load	109.0	78.6	109.2
			Peak-load	191.1	109.3	166.7
	Option III	9,810	Off-peak	55.2	55.2	62.5
			Mid-load	108.4	77.3	108.6
			Peak-load	178.7	101.0	155.5

Table 1. Electric rates table for general service (B) at different time period.

1.1.2.2 ESS for renewable energy

Not only for the peak shaving advantages, the effect of ESS can be increased at renewable energy field. According to the environmental challenges such as greenhouse gas effect, the importance of renewable energy is increasing globally. In case of California, USA, Govenor Edmund G. Brwon, Jr. signed legislation to require 50 percent of the state's electricity from renewable energy by December 31, 2030[3]. Also, government of the republic of Korea plan to replace 20% of power plant by renewable energy by 2030[4]. As shown in figure 2, the total capacity of renewable energy plant will be increased until 2030 and the ratio of solar and wind power energies also be increased.

However, these renewable energies such as solar and wind power have a problem of intermittent supply. For instance, if the weather is rainy or cloudy, the supply will be reduced compared with shiny day. Also, in wind energy, the power is dependent on wind speed and wind direction of the day. To solve these intermittencies, combination of renewable energy and ESS can be an efficient method to supply energy constantly and stably. As shown in figure 3, without ESS system, the natural supply of renewable energy shows intermittency and irregularity, however, by using ESS the renewable power shows stable and constant supply.

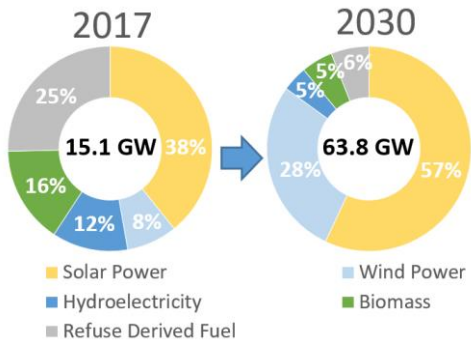

Figure 2. Renewable energy policy plan in Korea until 2030

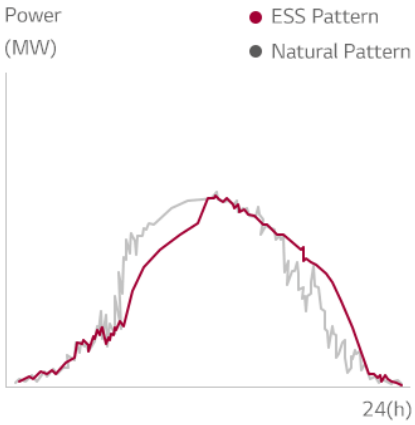

Figure 3. Integration of renewable energy by using energy storage system[5]

1.1.2.3 ESS for frequency regulation

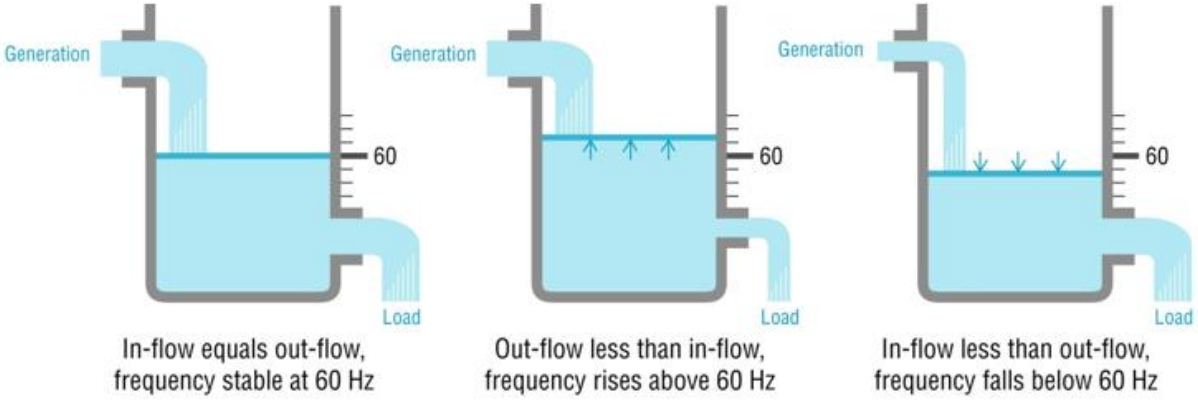

Figure 4. Power system frequency is like water flowing in and out of the bathtub. Joe Eto, Lawrence Berkeley National Laboratory[6]

It's important to maintain the rated frequency as 60Hz (±0.2Hz) in electrical power grid system in the republic of Korea. The constant frequency can be maintained when the demand and supply can be balanced at real time. According to Joe eto, the relation between electrical power and frequency can be explained by figure 4. The height of water in bath tub can interpret as frequency, water input and output can be interpreted as supply and demand. If there is a difference between supply and demand, the rated frequency is also changed. To explain simply, when the load is less than the generation, the frequency increase like figure 3 and vice versa, the frequency decrease. The problem is if the frequency difference is increase highly, it can cause problems such as a large scale black out phenomenon. In this case, using ESS can regulate this frequency because ESS which consists of battery can fast charge and discharge (ms unit) to regulate the frequency. In the republic of Korea, 52MW of ESSs are built at 2014 and 184MW of ESS at 2015 for frequency regulation. The number of ESS for frequency regulation have been increased until 2014,

Year	2014	2015	2016	2017	Total
Capacity (MW)	52	184	140	124	500
Number	2	7	4	4	17

Table 2. ESS for frequency regulation construction plan in the republic of Korea[8]

In the republic of Korea, coal power plants are operated while decrease its power by 5% for frequency regulation. Therefore, if that deficiency can be replaced by ESS, more pecuniary advantages are expected nearly 500,000,000 won per year.

1.1.3 Candidates of ESS

As mentioned at previous chapter, there are several functions of ESS. Not only for peak shaving, combination with renewable energy, also ESS has more functions such as offering ancillary services at both the transmission and distribution voltage levels.[9] According to these applications of the ESS, the requirements of ESS are also changed. For example, in peak shaving, the power of ESS is more important rather than the capacity because it should replace the power of power plant during peak time. In other case, used at energy independent house which is combined with renewable energy, the total capacity of the ESS is relatively more important. Therefore, it is significant to understand the requirement properties for different applications and compared with various kinds of energy storage systems. In this chapter, several energy storage systems will be introduced, and each system has different properties and characteristics.

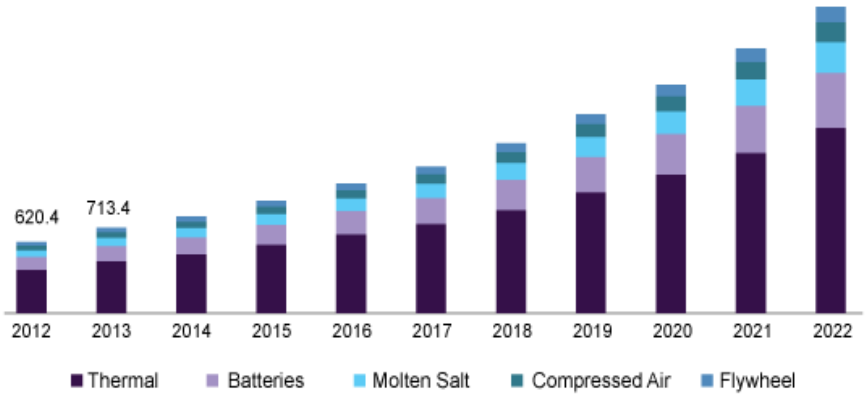

Figure 5. U.S. advanced energy storage systems market revenue, by technology, 2012– 2022 (USD million) *Grand view research, 2018

1.1.3.1 Thermal energy storage system

According to figure 5, thermal energy storage systems are the most occupied system in US energy storage market. During charging, the system store heat energies from solar or geothermal heat and releasing the heat during discharging. Advantages of using this system includes the high overall efficiency and reliability and better economics, reductions in investment and running costs, and less pollution of the environment, fewer carbon dioxide (CO_2) emission.[10,11] Among the thermal energy storage system, concentrated solar power (CSP) is most typical because of easy accessibility of combination with solar energy. CSP concentrates heat energy by focusing mirror at certain point, heat the molten salt and these salts are transported to ‘hot salt’ tank and ‘cold salt’ tank to store and use the energy.

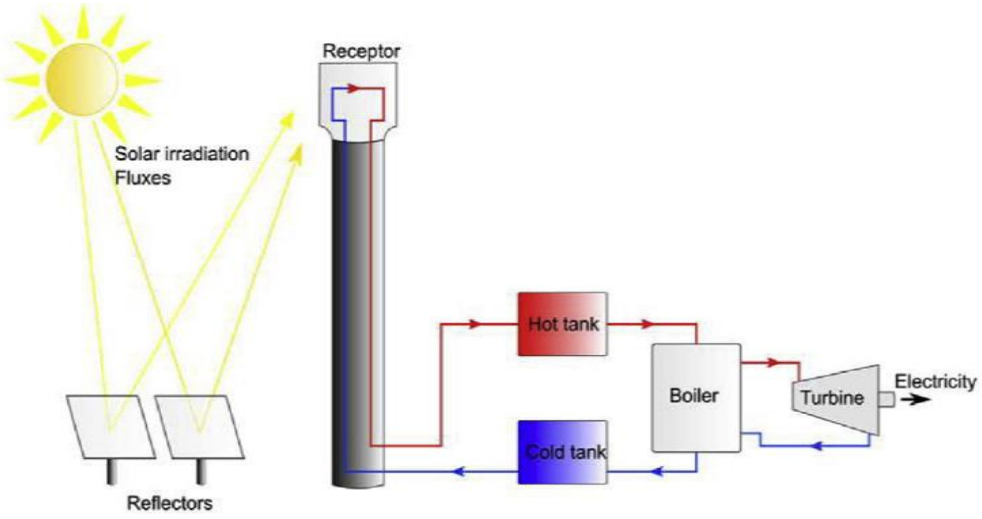

Figure 6. Scheme of thermal energy storage system[12]

1.1.3.2. Lithium-ion battery

Li-ion battery is most conventional energy storage system. The commercialized battery which is used as electric vehicle, use Ni-rich NCM ($Li[Ni_xCo_{(1-x)/2}Mn_{(1-x)/2}]O_2$) or NCA (NCA $LiNi_{1-x-y}Co_xAl_yO_2$) as cathode material. Also, they use carbon-based material as anode such as graphite and used liquid electrolyte. In the case of Li-ion battery, due to high development, it shows high power, capacity and cycle life compared than other battery systems. However, Li-ion battery is vulnerable to thermal stability because of using organic electrolytes. In 2018, there were several fire problems about ESS occurred in the republic of Korea.[13] The reason for the accidents is not Identified but Li-ion battery at high temperature could raise the accident bigger.

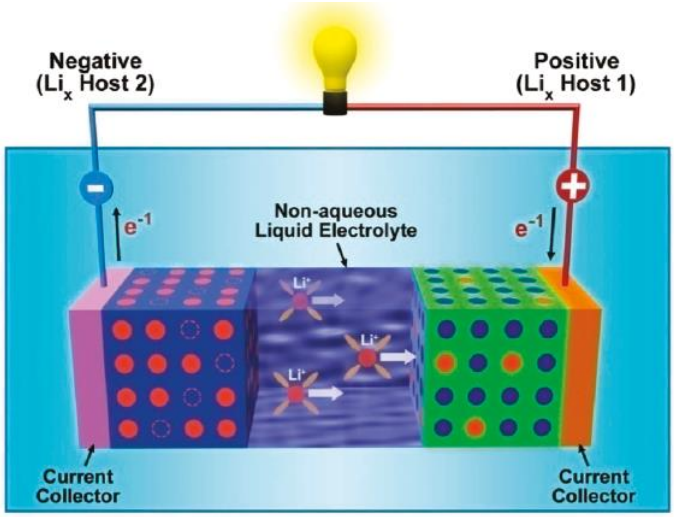

Figure 7. Scheme of Li-ion battery

1.1.3.3. Sodium Sulfur (NaS) Battery

The components of NaS battery consists of sulfur compound as cathode, sodium metal as anode material and Beta alumina ceramic as electrolyte. As shown in figure 8, beta alumina blocks contact between both electrode and during charge-discharge sodium ions are transported through this beta alumina ceramic while electrons are transported through outer circuits. The main characteristics of NaS batteries are stable long cycle life (4500 cycles expectation) by using solid electrolyte and cost advantages of using sodium metal.[14] However, in September 2011, the manufactured NaS battery exploded and the NGK company expected the cause of the exploding is short circuit by molten salt which is leaked from battery crack. Therefore, the company have been enhancing the safety issues of batteries such as constructed fuse between modules.

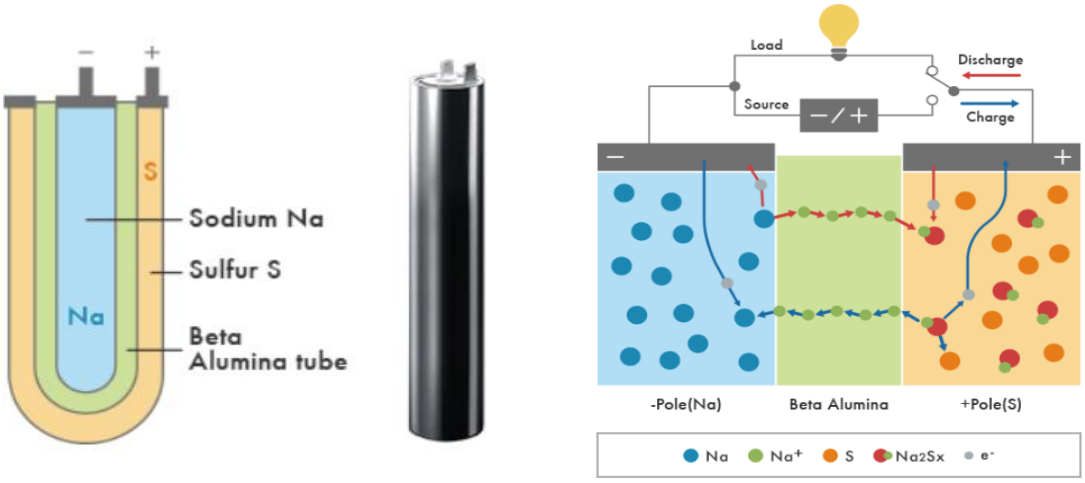

Figure 8. Scheme of NaS battery from NGK and operating mechanism of NaS battery

1.2 Liquid Metal Battery (LMB)

Liquid metal battery consists of two liquid metal electrodes and molten salt electrolyte. The first concept of LMB is originated by electrometallurgy which purify aluminum metal. The below graph briefly explains about history of liquid metal battery.

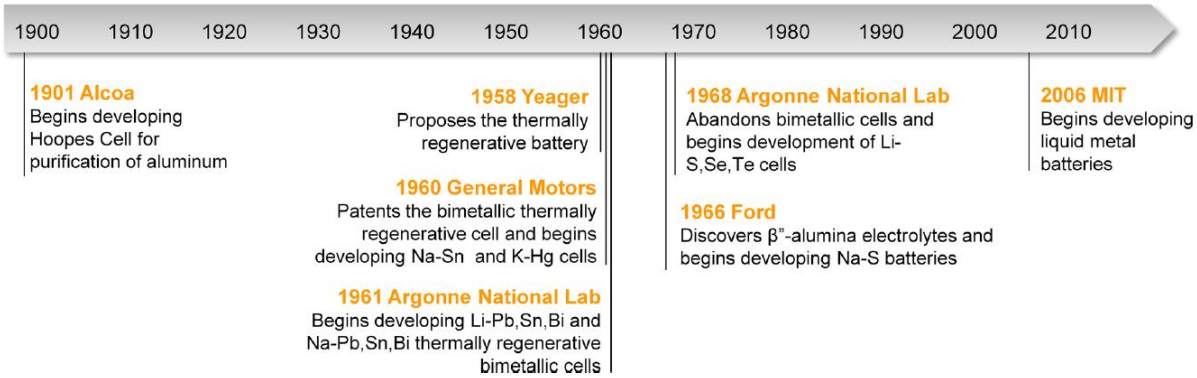

Figure 9. Historical timeline of the development of liquid metal battery[15]

Aluminum purification started using Hoopes cell at 1901 and the batteries using this electrometallurgy concept manufactured at 1960s. After several attempts to make battery systems at 1960s, the group of prof. Donald Sadoway started the research in MIT at 2006 and through Mg|$MgCl_2$-KCl-NaCl|Sb composition, they published the paper about liquid metal battery at the Journal of the American Chemical Society.

1.2.1 Principles of LMB

The all active materials of liquid metal battery are all liquid state and each component is self-separated by density difference and immiscibility. In this case, molten salt electrolytes have 2 functions. First function is electrolyte function which transport ions during charge-discharge and second one is separating two electrodes from contact which causes short circuit voltage. Therefore, the density of each component is very important in liquid metal battery system, so the candidates of each cathode and anode materials are limited by density difference. As shown in figure 10, the candidates of anode materials are located at the left side of periodic table which has low density and the cathode materials are located at the right side which has higher density value. Therefore, the electrolyte should have intermediate density between cathode and anode materials.

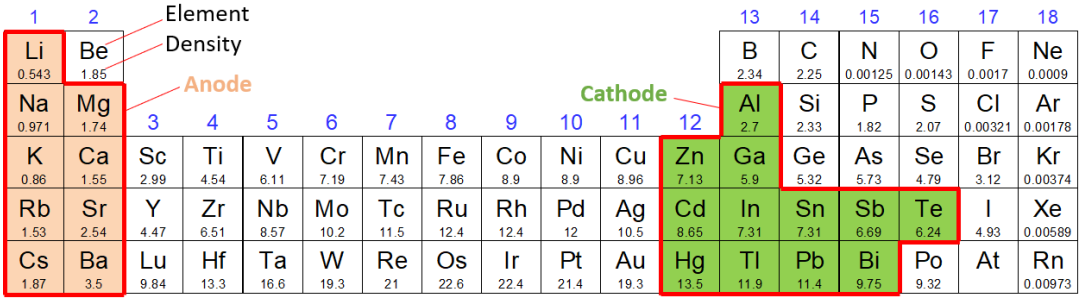

Figure 10. Candidates of negative (left) and positive (right) electrode for liquid metal batteries[15]

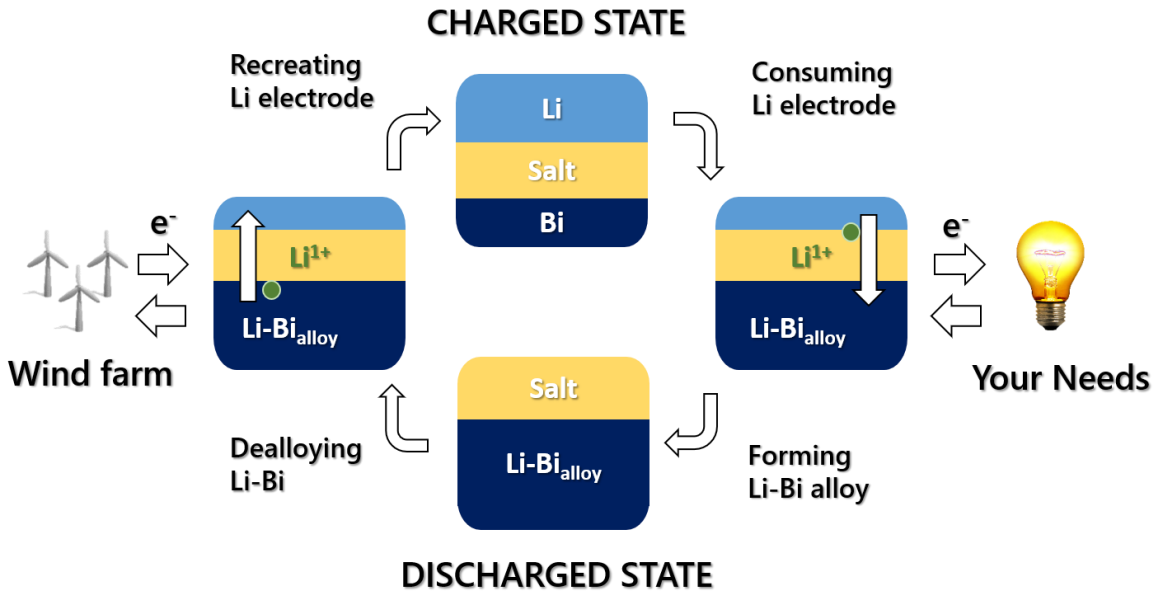

Figure 11. Schematic diagram of LMB during charging and discharging

Figure 11 explains the concept and charge-discharge mechanism of liquid metal battery. For instance, the heavy bismuth metal is used as cathode which has 9.75 g/cm^3 density and light Li metal is used as anode which has 0.54 g/cm^3 density. In the case of electrolyte, lithium-halide molten salts compounds which has intermediate density between anode and cathode are used as electrolyte to transport Li ion during charging and discharging. After melting all the components, the three active material components are self-separated by density difference and this state is charged state. During discharge, the lithium metal oxidizes to Li cation and the rest electrons move through the outer circuit and fulfill our needs such as light bulb and the Li cations move through molten salt electrolyte and they are reduced to Li metal at cathode and form Li-Bi alloy. The discharge process continues until the lithium-bismuth alloy cannot form anymore because

of limited mole fraction of lithium in bismuth or lack of lithium metal and that state is full-discharged state. During charge process the Li-Bi alloys become de-alloyed and Li oxidizes at cathode part and they are reduced at anode part by forming Li metal.

1.2.1.1 Advantages and Disadvantage of Liquid Metal Batteries

Nowadays, metal electrodes are widely used in battery systems and they are usually used as the form of solid states. Compared with solid metal electrodes, liquid electrode possesses the following merits:

(1) No dendrite formation during electrodeposition process;
(2) No phase deformation or grain size change during charge/discharge;
(3) Ease of building stable electrode/electrolyte interfaces and fabricating cells.

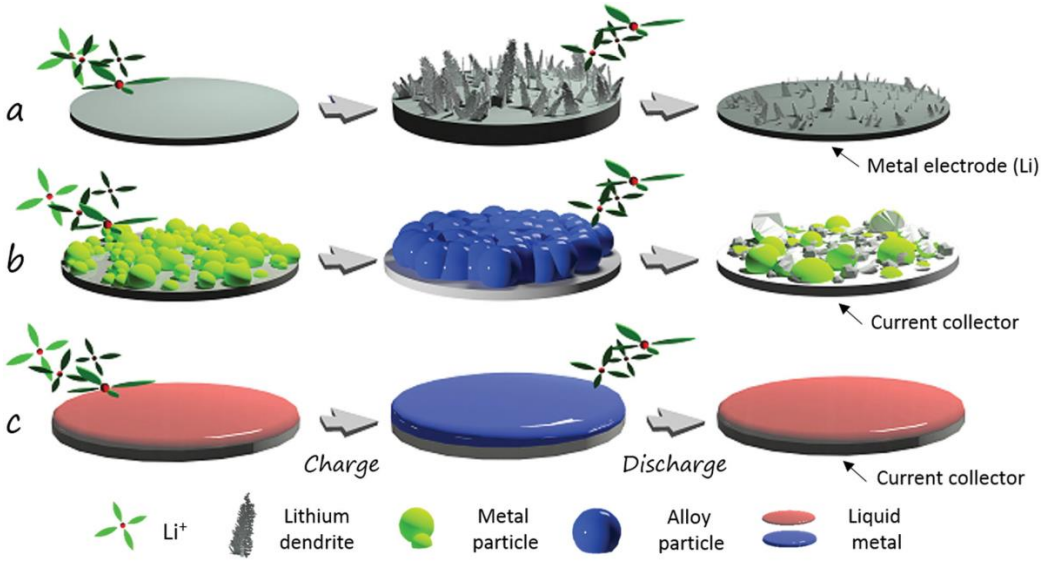

Figure 12. Schematic illustrating the morphology/structure changing of solid (metal plate electrode (a), metal/alloy composite electrode (b) and liquid metal electrodes (c) during charging/discharging.[16]

As shown in Figure 12(a), electrochemical process on metal electrodes can result in dendrite formation and structure collapsed. However, as shown in figure 12(b), (c), using liquid electrodes can avoid such deleterious electrode deposition process. Thereby they are safely operated for long service lifetimes according to the self-healing function of the liquidity. Besides, the liquid state of the electrodes can affect the manufacturing process of the battery system which related with capability for scale-up and the cost of batteries.[16] For example, the flow battery with liquid

electrodes is easier to scale up than lithium ion batteries with solid electrodes. The simple manufacturing process and excellent scalability of liquid-electrode-based batteries show great potential for large-scale energy storage application.

In the case of liquid metal battery, not only for electrodes, electrolytes are also liquid state so that it has fast ion transport and charge transfer properties.[15] However, most LMBs only work at high operating temperature (> 200°C). A high operating temperature corresponds to high vapor pressure of liquid metals and electrolytes, high cost of the secondary battery materials, and more obvious corrosion issues. Moreover, manufacture the long-term hermetic seal at high temperature is difficult because most of the polymeric seals usually cannot survive over 200 °C. The other problem of LMB is low operating voltages. The cell equilibrium voltage is related to the change in partial molar Gibbs free energy.[15]

$$E_{cell,eq} = - \Delta G_{cell}/(zF) = -(RT/(zF))\ln a_{A(\text{in B})} \quad [1]$$

where F is the Faraday constant and z the number of electrons. Conceptually, the thermodynamic driving force for cell discharge can be interpreted by a strong interaction of metal A with metal B, in which the activity of A can be extremely low ($a_{A(\text{in B})}$ can be low as 10^{-10}) and this is the main reason for the low equilibrium cell voltage.

1.2.2 Research Trends of Liquid Metal Battery

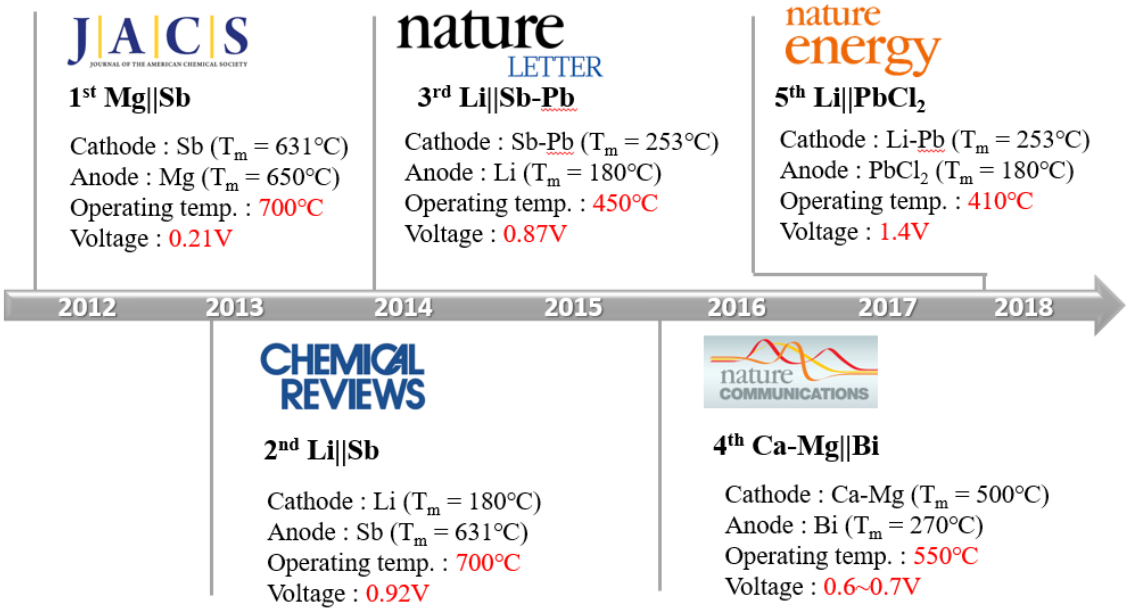

Figure 13. Research trends of liquid metal battery by published paper from prof. Sadoway's group

In figure 13, there are papers about liquid metal battery which published from 2012 to until now. The research trends focused on to solve the problems; decrease the operating temperature and increase the operating voltages. Finally, at 2018, the operating temperature of the LMB cell could be nearly 410°C and the operating voltage is nearly 1.4V. Compare with the first LMB composition, the performance of the cell has been developed at lower temperature.[15, 17, 18, 19, 20]

1.3. Research proposal

1.3.1. Objective of study

Liquid metal battery can be a candidate of energy storage system because of high current density, stable and long cycle life with no capacity fade and easy to scale up. However, compare with other battery systems, there was no standard test conditions such as cell design and test process, so it was difficult to evaluate the properties of active materials. Here, in this study, we constructed the standard test condition of liquid metal battery system and through the standard condition, we compare the active materials especially molten salt electrolyte, which was not evaluated before from other studies.

1.3.2. Cell design and optimization for liquid metal battery

In the case of liquid metal battery, there was several studies about active materials, however, a little information about passive materials are discovered such as current collector, cell container material and cell test furnace. In previous study, our group tried to set up the standard test condition of liquid metal battery and manufacture all the components and zigs. However, in real operating, there were other problems such as intermittent voltage drops and short circuit voltage. According to these studies, consider the factors which affect the voltage profile of liquid metal battery and methods to enhance the performance of the test cell.

1.3.3. Low operating temperature LiCl-LiI-KI molten salt electrolyte for liquid metal battery

After cell design and optimization, through the standard condition of the liquid metal battery we could make reference cell data. Compare with reference data with newly tested material, we could evaluate the properties of new active material. Here we choose LiCl-LiI-KI, Li-based molten salt electrolyte and test the intrinsic properties and cell properties with Li|LiCl-LiI-KI|Bi composition and compare with LiCl-LiI electrolytes.

2. Cell design and optimization for liquid metal battery

2.1 Previous studies

As mentioned in previous chapter, the concept of liquid metal battery as a secondary battery was first proposed from Massachusetts Institute of Technology (MIT), prof. Donald Sadoway's group at 2012[17].

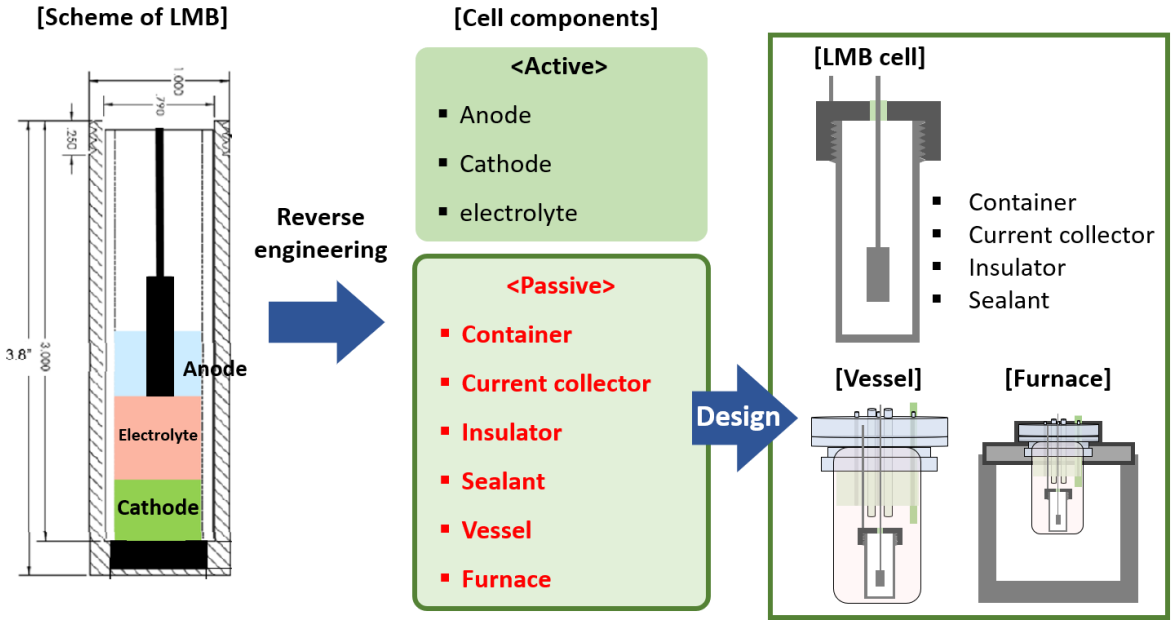

Figure 14. Reverse engineering process of LMB in our group

As shown in figure 14, from the scheme of prof. Sadoway group in MIT[17], the information of active materials such as anode, cathode, and electrolyte are well known however, the detailed information about passive materials such as container, current collector, and sealant is difficult to obtain. Therefore, according to the papers and patents of LMB cell we have to do reverse engineering. Thus, in previous studies in our group try to make main components such as cell container (SUS 304, stainless), Ni-Fe foam negative current collector and customized Ar gas flow test furnace.

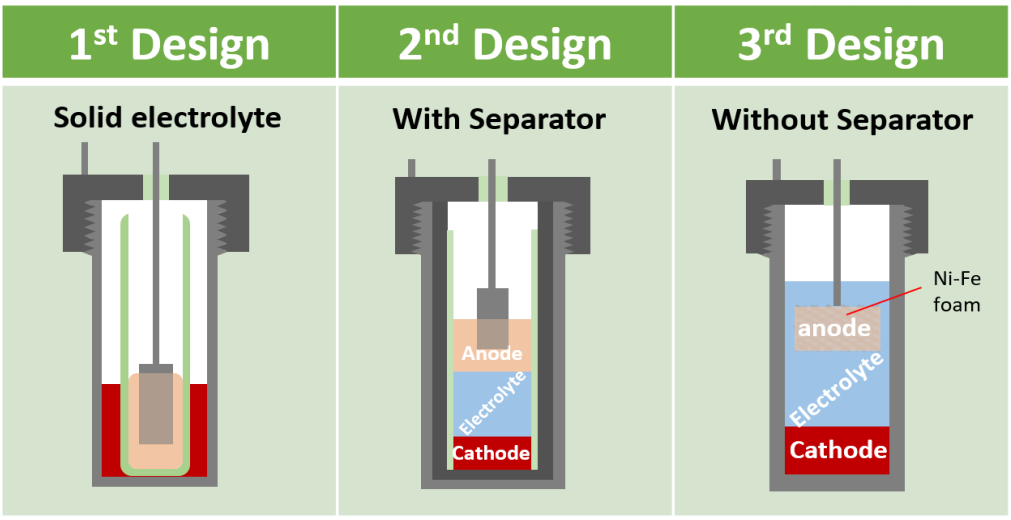

Figure 15. Change of LMB cell design in our group

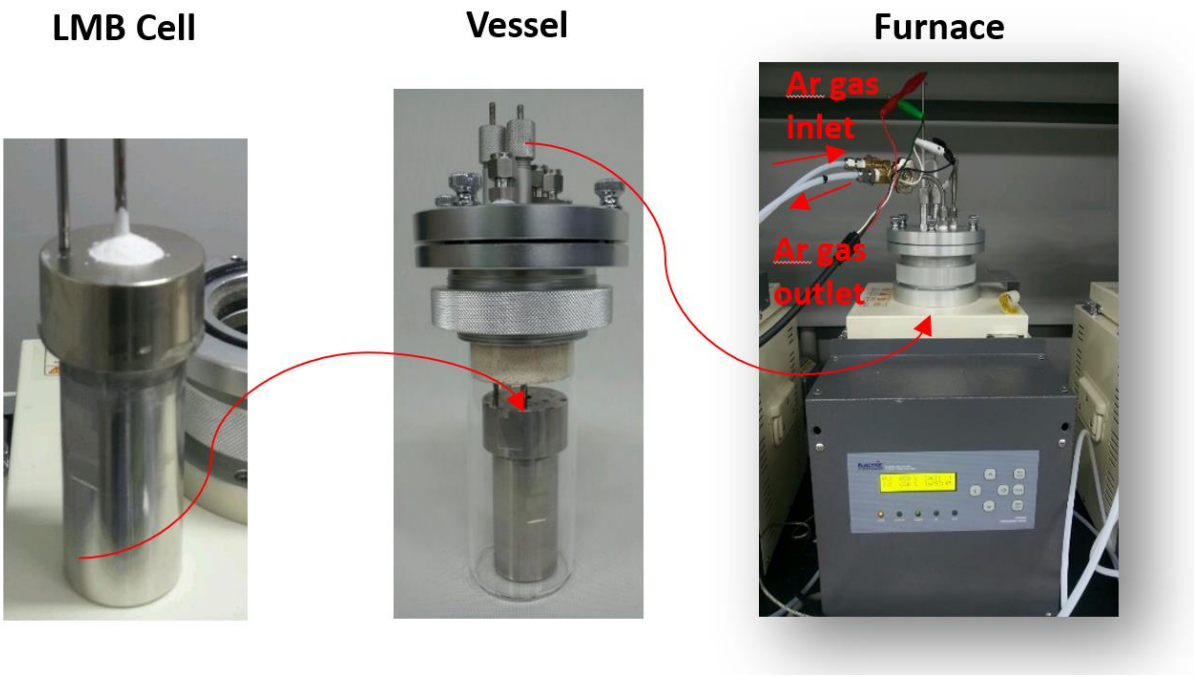

Figure 16. Cell design and fabrication in our group study

Also, the cell design changed by the sequence which appeared in figure 15. In the case of first design, the cell operated using solid electrolyte which is similar with NaS battery design. However, the problem of this design is over the 20mA current, cracks occurred at the beta alumina solid electrolyte. Because one of the main advantages of liquid metal battery is high current density, this design is considered as not proper to liquid metal battery system.

In the case of second design, molten salts are used as electrolyte and graphite is used as current collector. To prevent contact with anode and graphite current collector which cause short circuit voltage, alumina ceramic tube is used as insulator. However, due to the problem of side reaction

of liquid Mg anode and alumina or liquid Li anode and alumina, we consider this design is no proper to stable cycle data.

In third design, remove the alumina insulator which cause side reaction of anode material and using Li immersed Ni-Fe foam negative as current collector to exist Li metal inside the molten salt electrolyte. The negative current collector and positive current collector at the top part of cell container is insulated by alumina ceramic paste, however, the cell is not sealed from gas permeation because it has screw threads on top part. Therefore, as shown in figure 16, this design needs Ar gas flow test vessel and customized furnace by setting LMB cell in the test vessel inside customized test furnace. As shown in figure 17, this 3rd designed cell with Li|LiCl-LiI|Bi-Pb composition operates over 1000 cycle with small capacity fade.

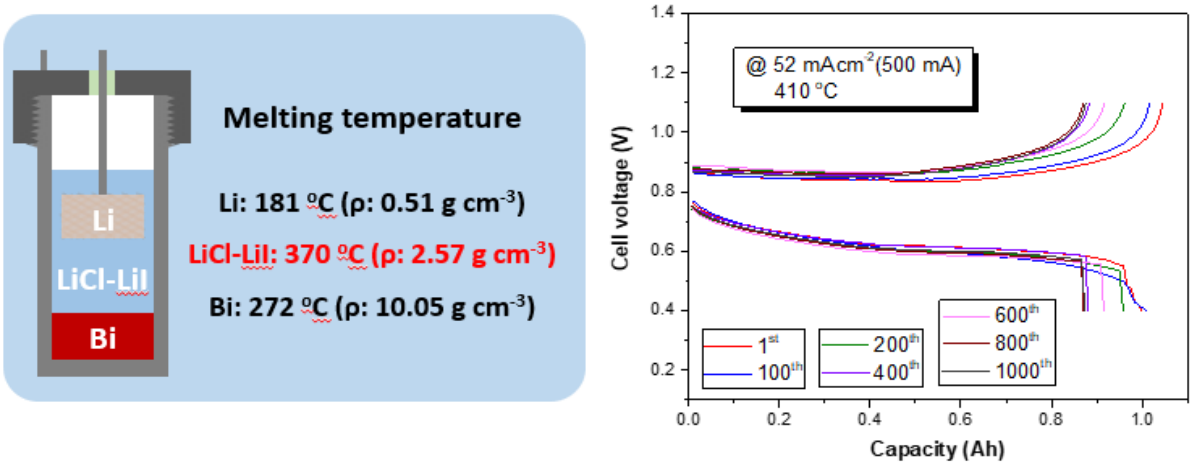

Figure 17. Composition of LMB cell using 3rd design and cell cycle performance data at 410ºC

However, the problem is not every LMB cell shows the same results such as voltage profiles and electrochemical properties. Furthermore, half of cell stop operating because of unstable voltage and unable to charge-discharge. For this reason, we have to consider all the factors which affect the performance of the LMB cell and optimize the factors with set up reference data. Therefore, we separate the factors which cause problem of testing LMB as two part.

1) Repeatability factor
2) Unstable voltage factor

The problem of low repeatability in cell test means the tested cell doesn't show the same electrochemical properties such as capacity, internal resistance and voltage profile. Furthermore, we could not expect the cycle performance even if all the cells are made at exactly same process.

The problem of unstable voltage means the intermittent voltage drop during charging and the cell voltage approaches near 0V and could not operate anymore. This problem is directly connected with cycle life of cell which operate less than 100 cycles.

2.2 Repeatability factors in liquid metal battery

As shown in figure 18, different cell with same condition shows different properties such as capacity, voltage gap except open circuit voltage which is the intrinsic property of the materials. Therefore, to get the constant data at same condition we analyze and optimize all the factors which affect the voltage profile of the tested cell.

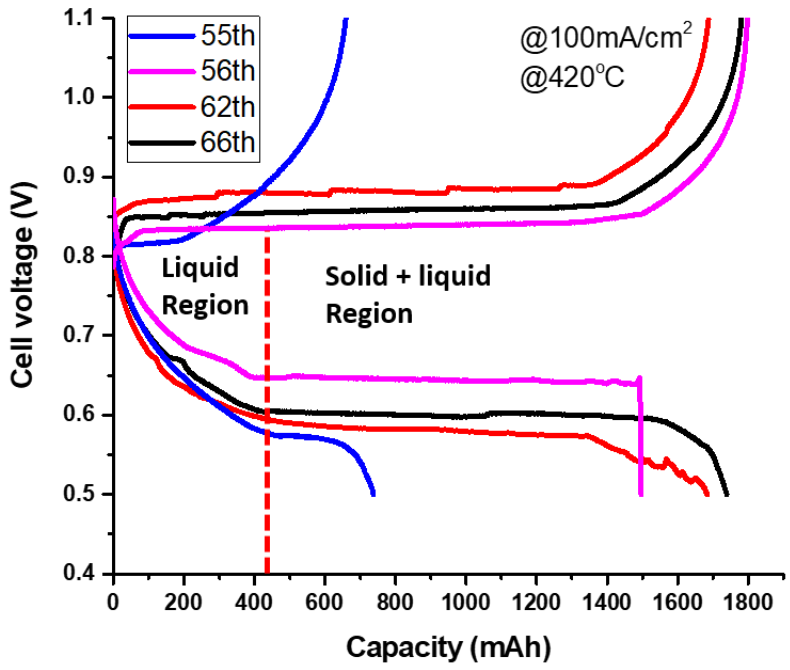

Figure 18. Voltage profile of Li|LiCl-LiI|Bi cell at various number of cells with same condition

1) Sealing factor

The first factor which affect the repeatability of liquid metal battery is sealing of the cell. In the previous designed cell, sealing of the cell which prevents the contact with moisture and outer atmosphere is not completely done. Therefore, flowing Ar gas is needed while operating LMB

cell in laboratory and this causes other problems such as contact with moisture when changing the exhausted Ar gas and also the flow rates of Ar gas can also affect the performance of cell. In addition, it provokes cost problems because we need to change the Ar gas (99.999% purity) per 2 weeks during operate the cell.

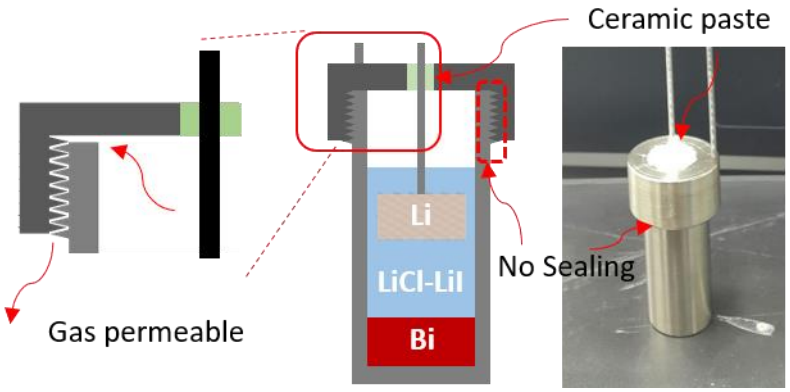

Figure 19. Sealing problem and gas permeation at previous cell design

As shown in figure 19, ceramic pastes are used at the top of the cell to separate negative current collector and positive current collector (SUS cell container) in the figure. However, there was a space between the cell lid and cell container although they are fabricated by screw thread. Therefore, this small space permits the gas transport and provokes electrolyte volatilization at high operating temperature.

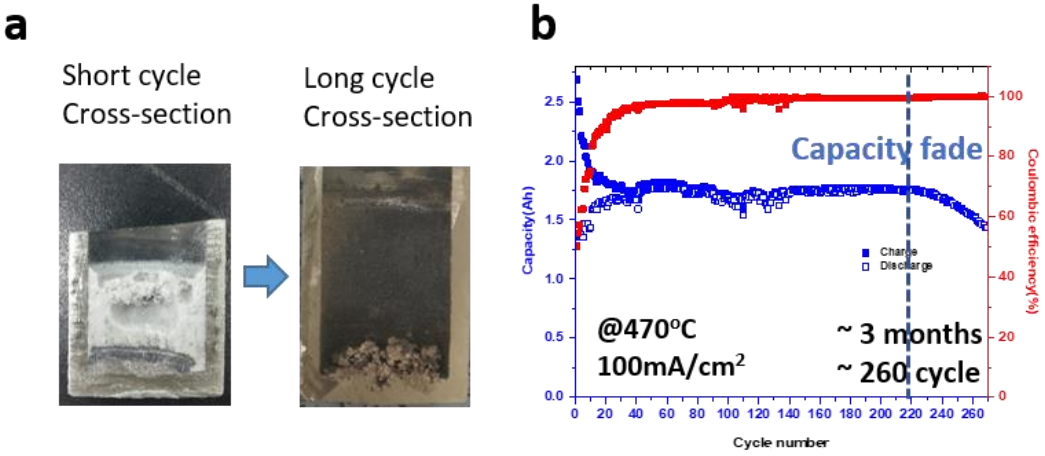

Figure 20. (a) Molten salt electrolyte (white part) volatilization at long cycle cross section, (b) capacity fade data at long cycle cell operation.

The right image of Figure 20(a) shows the cross-sectioned image after long cycle life with Li|LiCl-LiI|Bi composition as shown in figure 20(b). The operating temperature of this cell is 470ºC and current density is 100mA/cm^2. The cell operates over 260 cycles for 3 months, but capacity fade occurred after 220 cycles. The left cross-section image of figure 20 (a) shows large amount of rest electrolytes after short cycle life of cell. However, the right cross-section image of figure 20(a) shows small amount of rest electrolytes after long cycle with only metal part remained. According to these two images, there was an electrolyte volatilization in this design. Therefore, there's a need for the new design to prevent volatilization by sealing.

The study of LMB is actively researched by prof. Sadoway group of Massachusetts Institute of Technology (U.S.A) and prof. Kai Jiang group Huazhong University of Science and Technology (China) and both groups use the welding method as sealing the cell to make no gas permeability. Therefore, we try to solve sealing problem, we equipped Ar TIG welding machine in our laboratory and welded the cell for ourselves. This is because to minimize the contact of air and moisture during cell fabrication and test. Figure 21 shows the welding machine and welding booth of our laboratory.

Figure 21. Ar TIG welding machine and welding booth in laboratory.

As shown in figure 21, the LOK product and pressure gauge with LMB cell are fabricated before welding. Also, during welding the cell, Ar gas flows to prevent the contact with moisture and oxygen except the final process because at the process a small space of cell makes high pressure of Ar gas and it is difficult to weld at high Ar pressure. Using this process, the total exposure time will be less than 30 seconds.

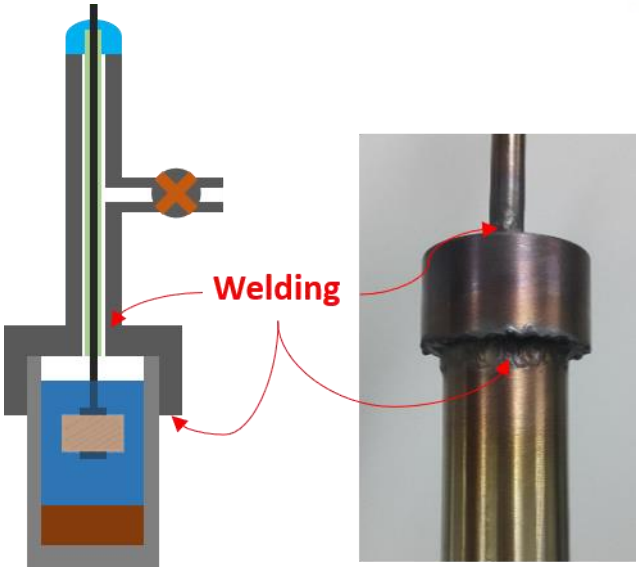

Figure 22. New welding design and welding part in SUS 304 cell in real experiment

Figure 22 shows the scheme of welding cell design and real cell figure after welding. The anode parts with Ni-Fe foam is fabricated to SUS 304 rod by nuts and the rod is also combined with an alumina ceramic tube by epoxy paste. These welded cells are tested after leakage test; paste detergent during Ar gas flow to maintain higher pressure than atmospheric pressure. If there are leakages, bubble will be formed at the leakage, so we could know the precise site of leakage in cell. Also, if there are no leakages at the cell, the test operates in this process in figure 23.

1) SUS cell sealing with Ar TIG welding

↓

2) Sealing test at positive pressure with bubbles

↓

3) Remove moisture dry the cell component at 80°C, 8h under vacuum

↓

4) Heated at 240°C for 12h under vacuum

↓

5) Purged with high purity argon gas (99.999%) and heated at 500°C for 5h

Figure 23. Ar TIG welding and cell testing process in laboratory

In Ar filled glovebox, put bismuth cathode and LiCl-LiI molten salt electrolyte and fabricated lithium anode. Before welding the cell, seal the screw thread gap by parafilm and after welding, maintain vacuum state at 80°C for 8 hours and increase the temperature at 240°C and maintain for 12h to remove the moisture and organic contaminant.[21] After these contaminant removal process, insert Ar gas and increase the temperature to 500°C (5°C/min) and operates the cell.

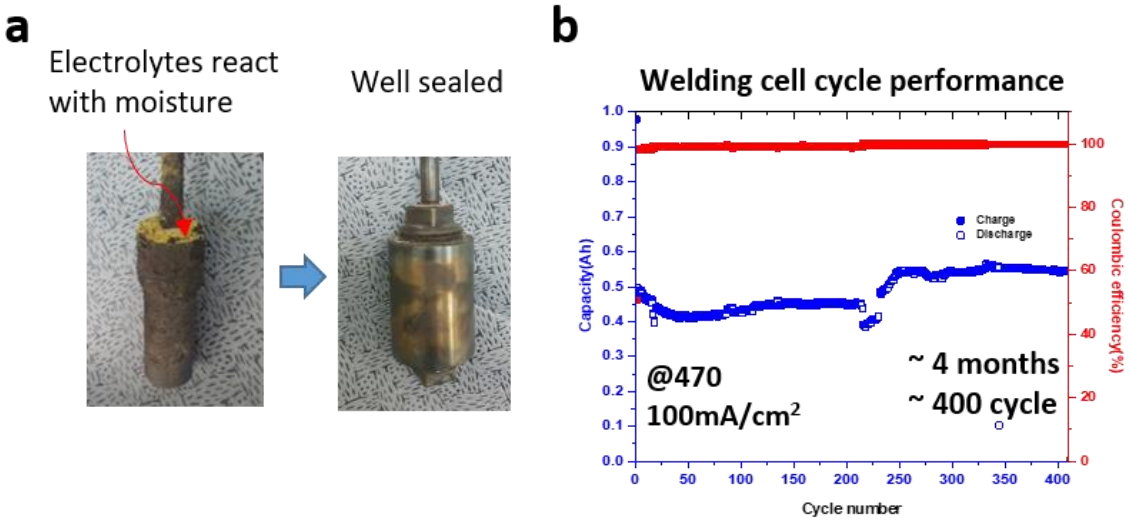

Figure 24. (a) Volatilization of electrolyte comparison after long cycle and (b) cycle performance of welding cell with Li|LiCl-LiI|Bi-Pb composition over 400 cycle

As shown in figure 24(a) if there is a leakage at the tested cell, the volatilization of electrolytes occurs and form yellow compound reacted with moisture. However, if the cell is well sealed, after long cycle life, no compounds are appeared even the operating time is over than 4 months, 400 cycles. According to figure 24(b) these well sealed cell shows stable cycle performance with no capacity fade over 400 cycles. Furthermore, the charge-discharge capacity increases in this cell, the reason of this phenomena can be explained as self-healing effect of liquid metal battery.[22] Because all the components are self-separated by density difference in liquid state so when the cycle goes on, the interface and each component get stable during charge-discharge process.

There is another advantage of using welding method to fabricate the LMB cell. Before using welding method, we must request to make SUS 304 cell container as customized design. However, the cost of these customized cell is expensive (~90 $). However, through welding method, we could make cell container by ourselves purchasing SUS pipe and SUS cap which is cheaper than customized cell (~9$) because it's just the market price. Figure 25 shows the self-made SUS 304 LMB cell container from market pipes and cap. Figure 25(b) shows the real tested cell after welding.

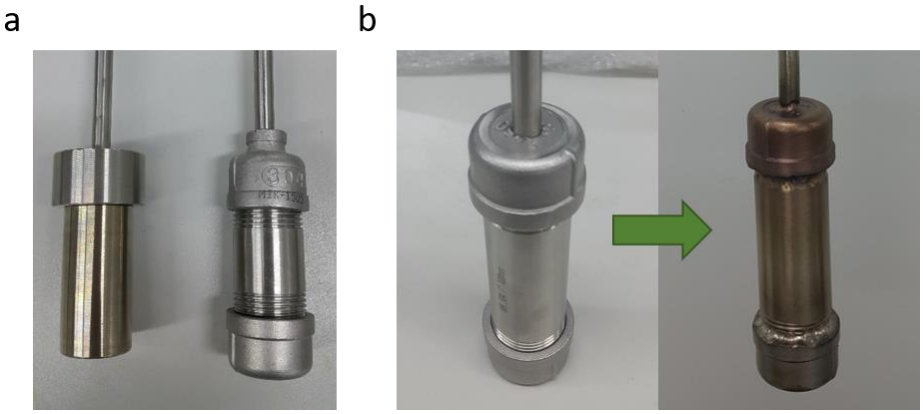

Figure 25. Comparison of customized cell and combined welding cell using SUS pipe and SUS cap (a) and real welding cell figure (b).

Also, in aspect of maintain cost, the test system doesn't need the Ar gas flow system because of no leakage, the cost of Ar gas is also saved. In addition, we don't need to make the customized vessel and test furnace to Ar gas flow, normal mini furnaces are used to test these welded cells.

2) Li immersion factor

As mentioned in previous chapter, lithium metal immersed Ni-Fe foams are used as negative current collector. In that case, the Li metal doesn't immerse in the Ni-Fe foam fully due to poor wettability of Ni-Fe foam with Li metal and this cause the capacity fade or in severe case, fail to operate. Also, the reason we consider this Li immersion problem as repeatability factor is because we could not expect the amount of Li metal which is immersed in Ni-Fe foam. This uncertainty can cause the difficulty of designing the ratio of cathode and anode.

Figure 26 shows the existing Li immersion process in negative current collector.

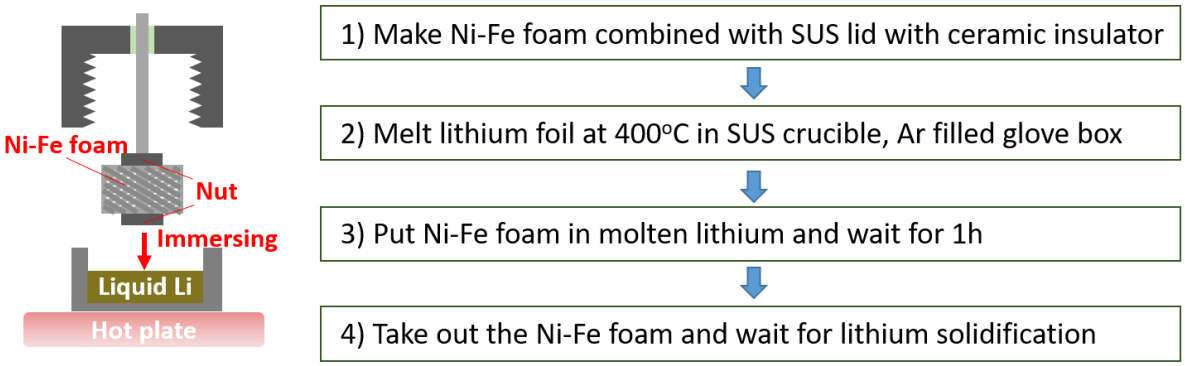

Figure 26. Previous lithium immersion method using hot plate in glove box

First, fabricate Ni-Fe foam, with SUS tube with two nuts and fix them with alumina tube through ultra LOK product and epoxy. Second, melt the Lithium foil in glovebox using hotplate at 400°C. And then put the fabricated Ni-Fe foam in the molten Li and wait for 1 hour as shown in figure 27(a). Finally take out the Ni-Fe foam from molten lithium and wait for cool down. However, the problem is it doesn't show the same amount of immersed lithium. As shown in figure 27(b) we tested lithium immersion experiment depends on the condition such as state of the glovebox (oxygen and H_2O ppm), state of the lithium metal (total exposure time in glovebox), temperature of hot plate and immersion time. The trends of Li immersion amount are proportional to low moisture, oxygen contents, high temperature and long immersion time and so on. Despite these trends of Li immersion in Ni-Fe foam, we could not get constant amount of Li anode. The temperature limit of hot plate is nearly 450°C and we could not use new lithium and new SUS crucible for every experiment. Decisively even at all the conditions are well prepared, we could not assure the Li immersion fully to the Ni-Fe foam. Therefore, we consider other method to immerse Li metal in Ni-Fe foam. This method is advised from prof. Hojong Kim in Penn State university in U.S.A.

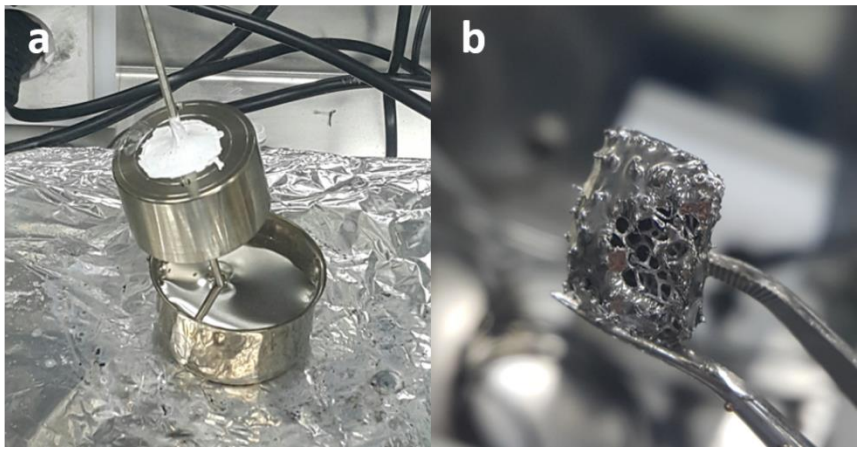

Figure 27. (a) Li immersion process using hot plate in glovebox and (b) the result of lithium immersion amount at 480°C for 1 hour

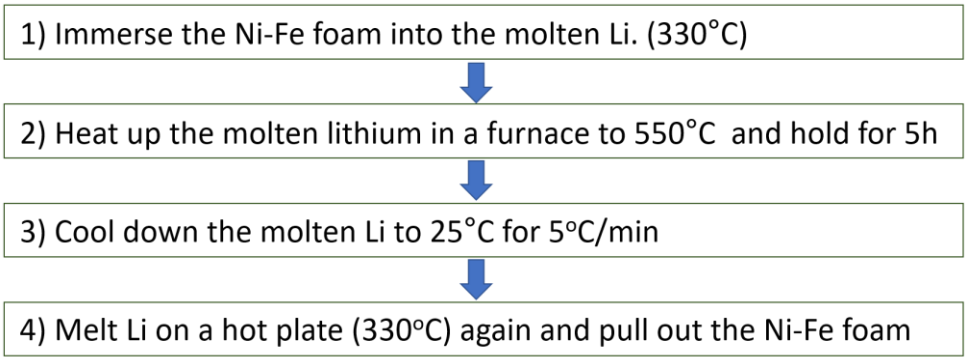

Figure 28. New process of Li immersion process on Ni-Fe foam

Figure 28 shows the new method to immerse Li in Ni-Fe foam. The main difference between previous method is fabrication of Ni-Fe foam with SUS tube after heating in furnace. According to the trends in previous conditions, the temperature of both Li metal and Ni-Fe foam is important. However, using hot plate applies heat at the bottom of the Li metal but the Ni-Fe foam is located at the higher part of molten lithium so it's difficult to transfer heat to the Ni-Fe foam. In the case of using mini furnace in glovebox, we expect the heat transfer evenly at both Ni-Fe foam and molten lithium.

Figure 29. (a) Li immersion process using furnace in glovebox and (b) the cross-section Ni-Fe foam result after heating in furnace

As shown in figure 29(a), mini furnace is used to immerse lithium metal in Ni-Fe foam in glovebox. Also, in figure 29(b), the cross-sectioned Ni-Fe foam shows the fully immersed lithium in Ni-Fe foam. Using furnace during Li immersion shows fully immersed Ni-Fe foam constantly regardless of the condition of glovebox atmosphere and lithium condition. Therefore, only consideration of the weight and volume of Ni-Fe foam is needed to expect the amount of Li anode design the ratio of cathode and anode materials. Also, due to this new immersion method, it's easy to expect the theoretical capacity of fabricated LMB cell.

3) Cathode wetting problem

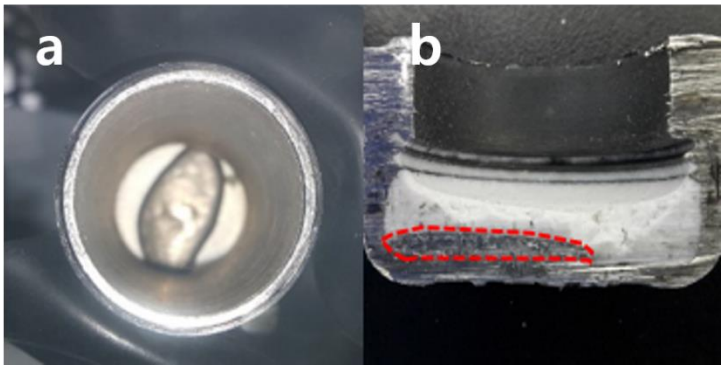

Figure 30. (a) Poor wettability of molten bismuth cathode on SUS 304 shows less contact region compare with full cathode current collector and (b) Cross-section image after cycle also shows poor wettability of bismuth metal on SUS 304 cell

As shown in figure 30, after melting bismuth metal on SUS 304, the metal doesn't spread on the whole area of SUS 304 bottom. This is because of poor wettability of bismuth metal and SUS 304.[23] This poor cathode wettability problem is considered as repeatability factor because the real active area or contact area is different at every experiment. In addition, this problem affects the current density or power density which are calculated data from active area.

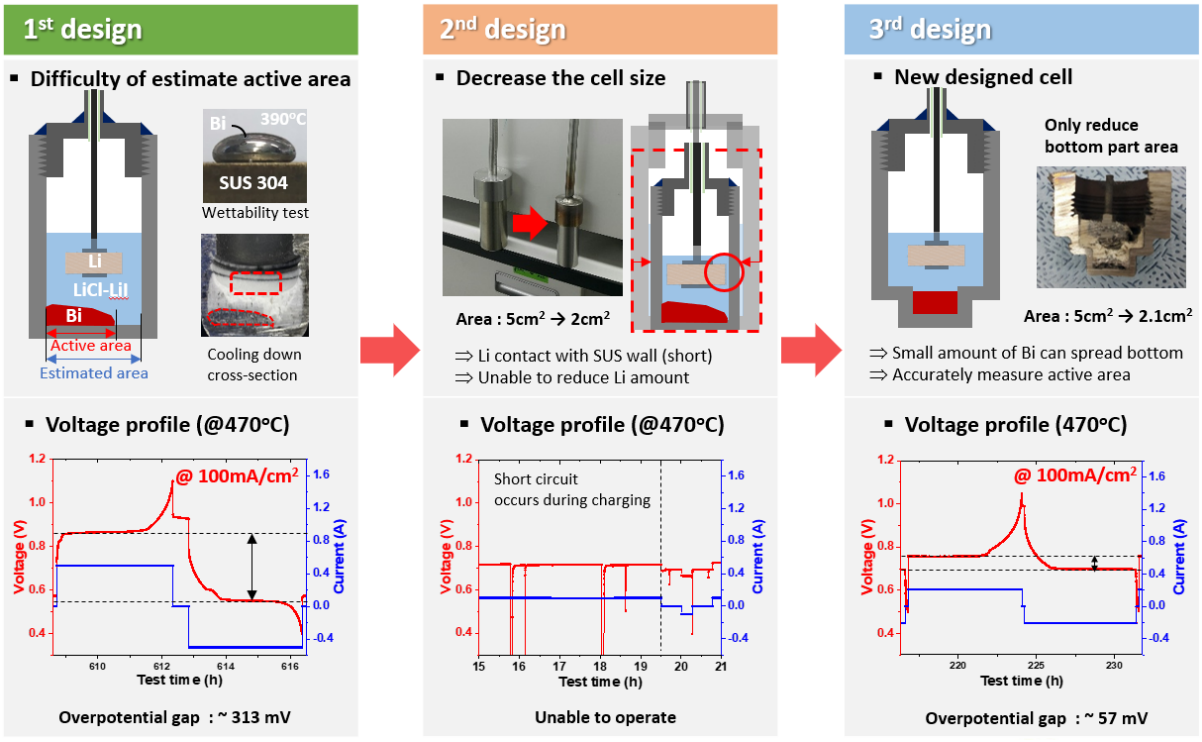

Figure 31. Strategy to solve cathode wettability problem by changing the design of the cell

Above figure shows the process of solving cathode wettability problem by changing the cell design. The first strategy for solving this problem is just reduce the cell area. When decrease the cell area from 5cm^2 to 2cm^2, short circuit voltage occurs during charging. We expect the reason of this phenomena is the contact of Li (anode) with SUS wall (cathode) because decrease of the cell area also decreases the distance from Ni-Fe foam and SUS wall. If the charged Li metal doesn't form inside of Ni-Fe foam, but the surface of Ni-Fe, it can cause the contact of Ni-Fe foam and SUS wall. The other method is maintaining the cell area but increase the amount of bismuth cathode material, but this also could not be the solution because to design the ratio of cathode and anode, the amount of anode should increase too.

Therefore, the next strategy is designing the cell with different area at cathode and anode. As shown in figure 31, 3rd design, maintain the cell area of anode part but decrease the cell area of cathode part. The decreased cathode part can fill the bismuth anode with all the active area and maintain the anode part area to prevent the short circuit voltage. Another advantage of this design is set up the criteria of active area. In the previous designs we set the cell area by cathode part whether the Ni-Fe foam area is smaller than cathode part. However, in this cell design we can clearly measure the active area by the reduced cathode area.
As shown in figure 31, compare the voltage profile of 1st design and 3rd design, at the same current density (100mA/cm^2), 1st designed cell shows much higher voltage gap (~313mV) than 3rd designed cell (~57mV). (the applied current of 1st design is 500mA, and 3rd design 210mA.) These results show the advantages of the new design which can measure the precise active area of the cell by utilizing the full area of cathode part.

2.3 Unstable short circuit voltage factors of liquid metal battery

In this chapter, we treat the problem of unstable short circuit voltage, the cause of the problems and its solutions. Figure 32 shows the standard unstable short circuit voltage problem of our liquid metal battery system where the voltage drops during charging. According to the several test, we verify this voltage profiles occurred frequently. The significant point of this problem is the voltage drop only occurs during charging. To find the reason of this phenomena we cross-sectioned the cell when the short circuit voltage occurs after cooling down the cell.

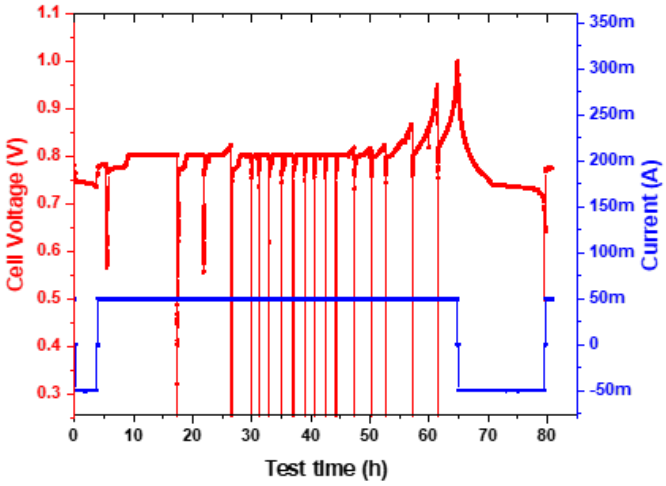

Figure 32. Unstable short circuit voltage profile for Li|LiCl-LiI|Bi liquid metal battery cell

.

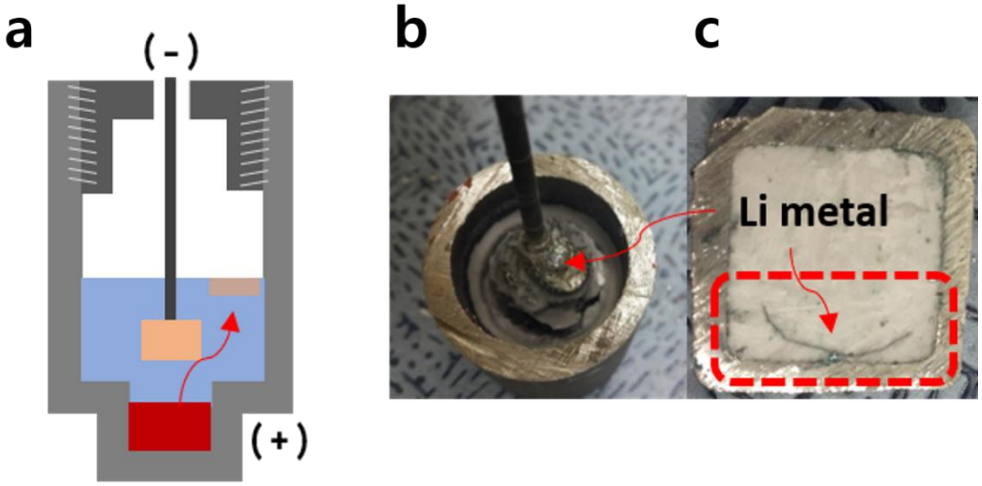

Figure 33. (a) Scheme of Li|LiCl-LiI|Bi LMB cell cross-section image which occurred short circuit voltage

As shown in figure 33(a) and figure 33(b), the main reason is the discharged lithium doesn't form inside but the surface or the top of Ni-Fe foam during charging.

To solve this problem, 3 methods are tested.

1) Size change of Ni-Fe foam
2) Control the height of electrolyte which locate the center of Ni-Fe foam
3) Design new furnace to prevent the tilting shaking of the cell

1) Size change of Ni-Fe foam

In the previous design, the width of Ni-Fe foam is longer than the height, so Ni-Fe foam get closer to the SUS wall. As shown in figure 34, the newly designed Ni-Fe foam reduce the width but increase the height which maintain the total amount of Li metal.

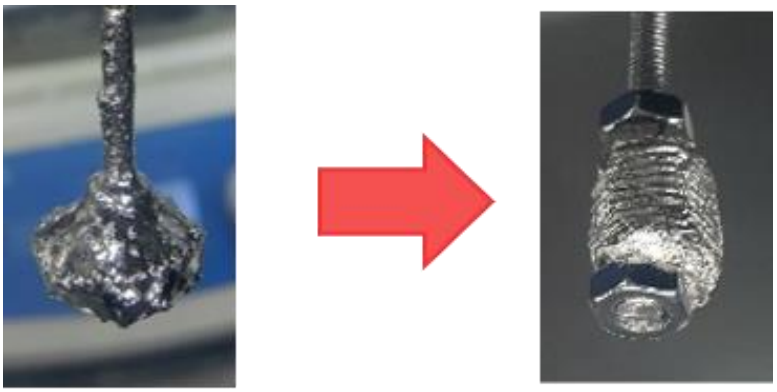

Figure 34 Size change of Ni-Fe foam to prevent contact with Li metal and SUS wall

2) Control the height of electrolyte which locate the center of Ni-Fe foam

The primary principle of liquid metal battery is the density difference of each active material. Therefore, Li metal must float on molten salt electrolyte because density of Li is less than molten salt. Applying this property to cell operating, we expect the height of molten salt electrolyte is located at the center of the Ni-Fe foam, reduced Li metal also is also located inside of Ni-Fe foam.

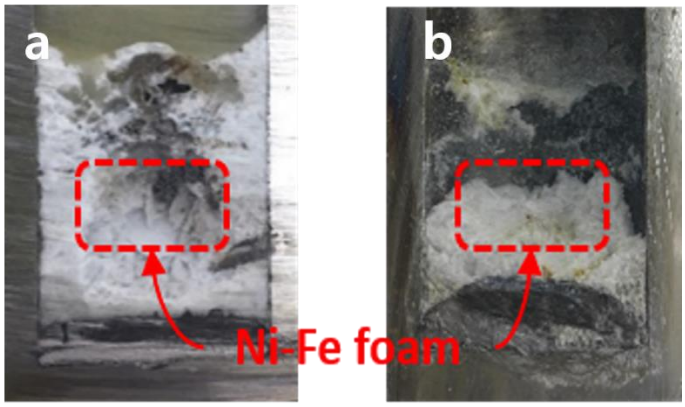

Figure 35. Change the electrolyte height proper to Ni-Fe foam to immerse the Li metal in to the Ni-Fe foam

As shown in figure 35, several tests are operated at various height of molten salt electrolyte to control the height of electrolyte.

3) Design new furnace to prevent the tilting shaking of the cell

Among the factors which affect the performance of LMB cell, shaking and tilting of the cell is also important factor based on constant experiments. In some case, if there is shake of the cell, voltage drop occurs even at well operated cell, however in the reverse case, poor operated cell can have a good cycle performance after shaking. Also, as shown in figure 33, in the case of charged lithium located on the Ni-Fe foam, tilting the cell can affect the performance of the cell, too. The reason for this phenomenon is also related in the contact of Li metal with SUS wall, short circuit voltage. Therefore, to minimize the effect of this shaking and tilting, designed a new furnace for LMB cell test. As shown in figure 36, the furnace design is changed from Ar gas flow design to new design which fix the cell by perfectly fitted area for cell size and furnace lid.

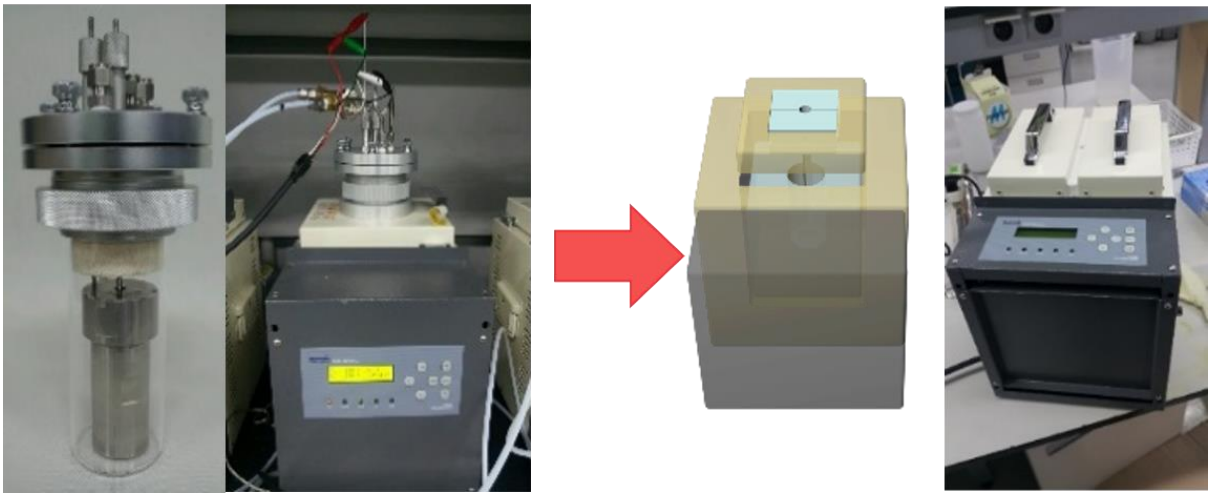

Figure 36. Change of furnace design from ar flow test vessel to new design furnace which can fix the cell from shaking and tilting

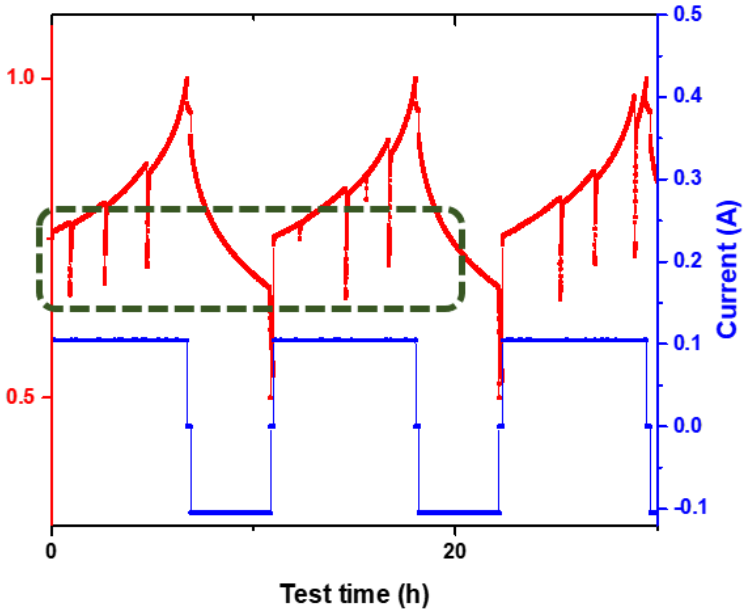

Figure 37. Voltage profile of Li|LiCl-LiI|Bi cell which applied 3 methods to prevent short circuit voltage

Despite all these methods to prevent the short circuit voltage of liquid metal battery cells, the voltage profile appeared as figure 37 still shows voltage drop. Voltage drop of figure 37 is moderated compared with previous voltage profile but it still shows the voltage drop at 0.7~0.8V. Consequentially, the previous 3 methods can contribute to reduce the voltage drop, but it could not be the fundamental solution for unstable voltage problem.

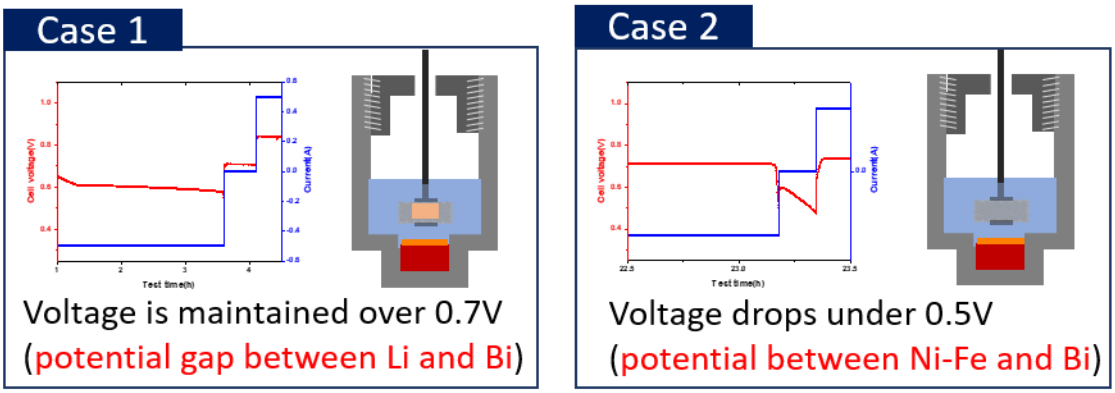

Figure 38. 2 case of open circuit voltage after full discharge

To find a new method to solve this problem, we could know that there are 2 case of open circuit voltage after full discharge. As shown in figure 38, the first case shows open circuit voltage over 0.7 V, but in the second case 0.5 V of open circuit voltage appeared. The reason for this voltage difference is in the first case the voltages are the potential difference between Li metal and Bi metal, however in the second case, at full discharge all the lithium gets out of Ni-Fe foam, so the voltages are the potential difference between Bi metal and Ni-Fe foam.

With these results, we expect the solution for stable voltage at operating is control the ratio of cathode and anode. In other words, if the Li metal don't fully get out of Ni-Fe foam at full-discharge, the charged lithium will form inside of the Ni-Fe foam. In the case of previous cells, the mole fraction of Li metal is less than the mole fraction of Bi metal so all the lithium metal can make alloy in the bismuth cathode and also theoretical capacity of cell is determined by the amount of Li metal. To increase the ratio of Li metal, the size of Ni-Fe foam should be bigger or reduce the amount of bismuth cathode. In this point, there are advantages of new cell design which moderate the cathode amount and Ni-Fe foam size limit. To increase the ratio of Li metal, reduce the amount of bismuth as half, but there was no cathode wettability problem in the cell test because of newly designed cell. Due to decrease of cathode material, the amount of cathode limited the total theoretical capacity of LMB cell and we called this concept of cell as cathode limited cell.

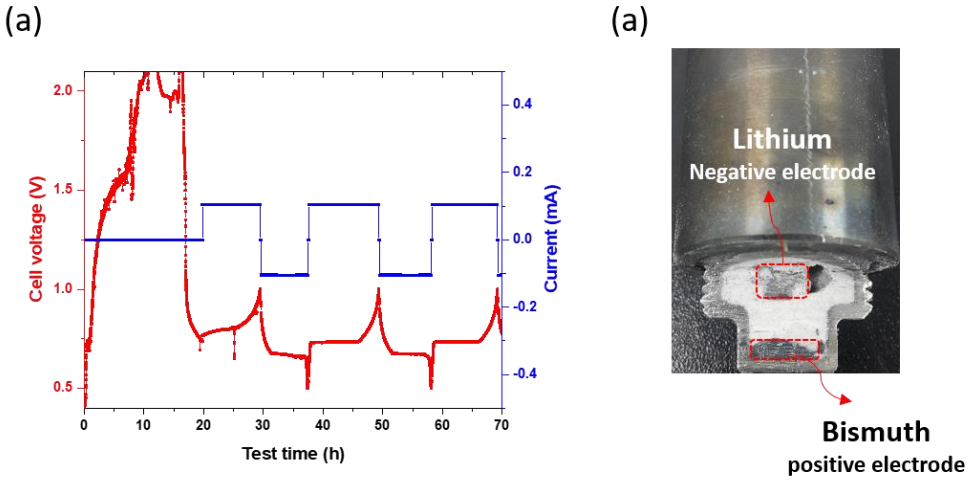

Figure 39. (a) 1st cycle of Li|LiCl-LiI|Bi cell after melting all the components at 470°C. (b) Cross-section image after full discharge

As shown in figure 39(a), in cathode limited cell, it shows stable cycle performance even in 1st cycle just after melting the components. The unstable voltage before 20 hours means the solid state of each material. There was a voltage drop in first charge process, but soon, it shows stable

charge-discharge. We expected the reason of this stable cycle is remaining lithium metal in anode part during full discharge. As shown in figure 39(b), to verify this expectation, cross-sectioned the cell after full discharge. In that figure, there was a lithium metal at the position of negative current collector, while previous design charged lithium metal was formed at the surface of the Ni-Fe foam as shown in figure 33.

.

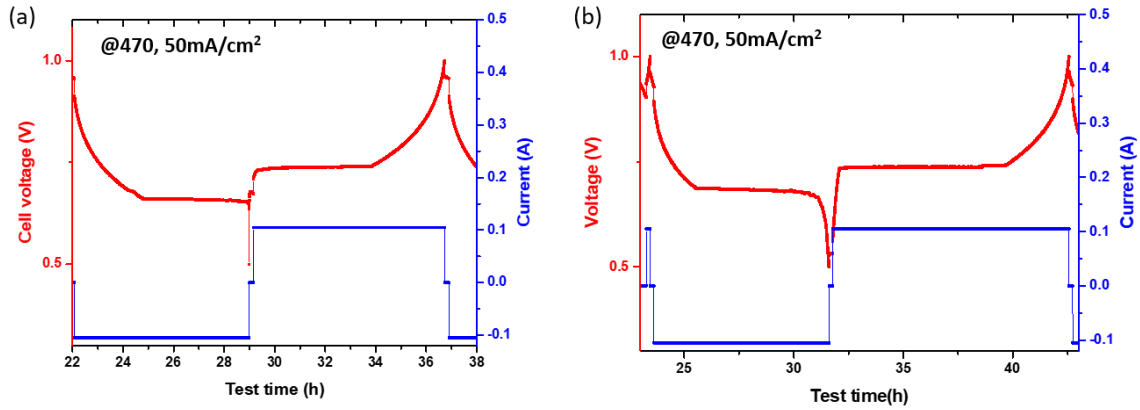

Figure 40. (a) Anode limited and (b) cathode limited Li|LiCl-LiI|Bi LMB cell voltage profiles

Also, verify with figure 40(a), in the case of anode limited cell, the mole fraction of Bi cathode is larger than Li anode, during full discharge the sharp voltage drops appeared in the graph near 29 hours of test time. However, in the case of cathode limited cell, figure 40(b), during full discharge the voltage decrease slowly compared with anode limited cell. In the former case, at full discharge, there was a depletion of lithium metal at anode and because of liquid state of cathode part, there was no kinetic limit to make slow reaction. However, in the latter case, during full discharge, bismuth cathode limited the kinetics of reaction. To be a full discharge in this condition, all the bismuth metal form the solid Li-Bi alloy. As the cathode becomes the solid state, more kinetic limits are occurred in the cell.

2.4 Summary

In this chapter, we consider the cell design of liquid metal battery and its test condition optimization. We organize previous works about optimization and the separate the problem as to factor, poor repeatability and unstable voltage. By optimizing these two factors, the tested cell shows constant voltage profile and cycle performance gradually. According to this optimized test system, we could also test other active materials and by comparing the performance with reference data, we could determine the properties of new chemicals.

3. Low temperature LiCl-LiI-KI molten salt electrolyte for liquid metal battery

3.1 Research Background

In previous chapter, we optimize the cell design and organize the test conditions of liquid metal battery system. Through the optimized reference data, the new material test will be done in this chapter. As mentioned in chapter 1, the problem of liquid metal battery is low operating voltage and high operating temperature. Here, in this thesis, we focus on the lowering the operating temperature of liquid metal battery.

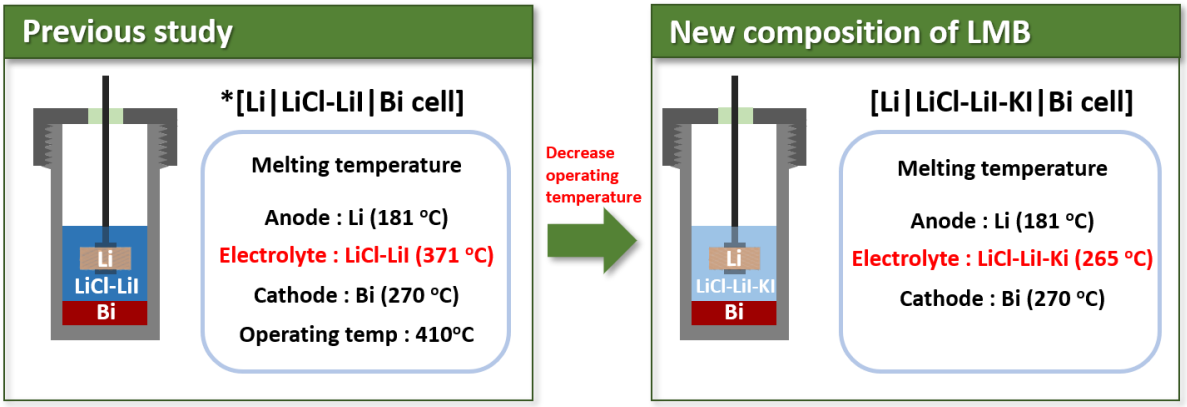

Figure 41. Lowest operating composition of LMB and process of decreasing operating temperature

The left scheme of figure 41, shows the lowest operating temperature composition of liquid metal battery based on Li metal anode.[23] the cell use anode as lithium metal, electrolyte as LiCl-LiI molten salt and cathode as bismuth metal. The melting temperature of each component is Li (181°C), LiCl-LiI (371°C), Bi (270°C) and the final operating temperature is 410°C. Because the melting temperature of LiCl-LiI molten electrolyte is relative higher than other active materials, so we expected if the electrolytes are changed to other materials which has lower melting temperature, the operating temperature will be decreased too.

Molten salt	300°C	350°C	400°C	450°C
LiCl-KCl	Solid state	1.0446	1.2947	1.5577
LiI-KI	0.8879	1.0783	1.2722	1.4672
LiCl-LiI-KI	1.0821	1.3035	1.5273	1.7508
LiF-LiBr-KBr	0.6916	0.9081	1.1449	1.3981

Table 3. Ionic conductivity of molten salts which has melting temperature under 350°C[24]

Table 3 shows several lithium based molten salt electrolytes which has melting temperature under 350°C. These molten salt materials are investigated as electrolytes for thermal activated battery systems which has a similar structure with liquid metal battery system. The previous molten salt electrolyte, LiCl-LiI has the lowest melting temperature among Li based halide molten salts. This means that to decrease the temperature of liquid metal battery system, multi-cation molten salts are needed such as molten salt which contain potassium ion as shown in table 3. Among the molten salts in table 3, LiCl-LiI-KI salt shows the lowest melting temperature as 265°C. Also, ionic conductivity of LiCl-LiI-KI molten salt at various temperature is relatively higher than other salts. For these reasons, we choose LiCl-LiI-KI salts for low operating temperature molten salts and tested its properties.

3.2 Intrinsic properties of LiCl-LiI-KI molten salt

Before applying the LiCl-LiI-KI molten electrolyte for liquid metal battery, it is important to identify the intrinsic properties of this molten salt.

Figure 42 shows the making process of homogeneous LiCl-LiI-KI molten salt.

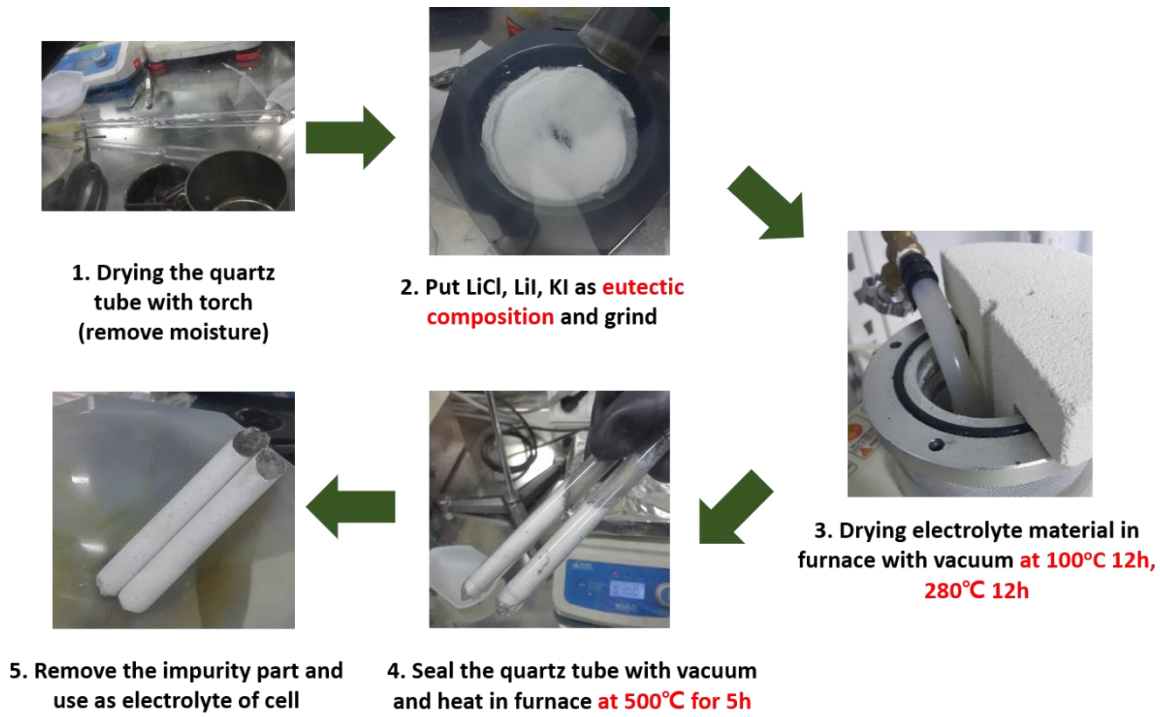

Figure 42. Making process of homogeneous LiCl-LiI-KI molten salt

1. Drying the inside of quartz tube with torch to remove moisture while vacuuming the tube
2. Grind LiCl (99.9%, Alfa aesar), LiI (99.95%, Alfa aesar) , KI (99.99%, Alfa aesar) as eutectic mole fraction homogeneously in Ar filled glovebox
3. Drying salts with vacuum in furnace at 100°C 12h, 280°C 12h to remove organic contamination[21]
4. After drying, seal the quartz tube during vacuum and heat at 500°C, 5h in furnace in glovebox
5. Remove quartz tube and impurity part from molten salt electrolyte

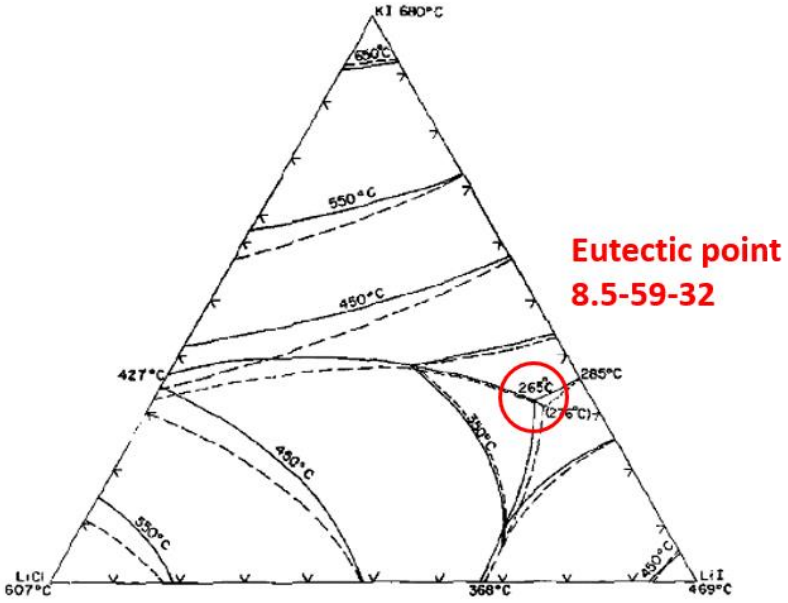

Figure 43. Phase diagram of LiCl-LiI-KI composition and eutectic point

LiCl-LiI-KI molten salts are synthesized at eutectic composition appeared as figure 43, LiCl-LiI-KI (8.5-59-32, mole fraction).

Before experiment to verify the properties of molten salt, we investigate the requirement of electrolyte for liquid metal battery to consider what properties are fulfilled as electrolyte of LMB.

The requirement of electrolyte for liquid metal battery is as following.[15]

1) Low melting temperature
2) Minimal metal solubility
3) No irreversible side reactions of spectator ions within the operating voltage window
4) A density intermediate between the positive and negative electrodes to facilitate the self-segregation of the three liquid layers
5) High ionic conductivity for high rate capability and energy efficiency

We tested LiCl-LiI-KI molten salt to verify whether it's proper to above requirements. Some tests need the detailed and precise equipment for measuring, so we found simple method to find trends of properties.

3.2.1 Melting point of LiCl-LiI-KI molten salt

The melting point of LiCl-LiI-KI molten salts are measured by Differential Scanning Calorimetry (DSC).

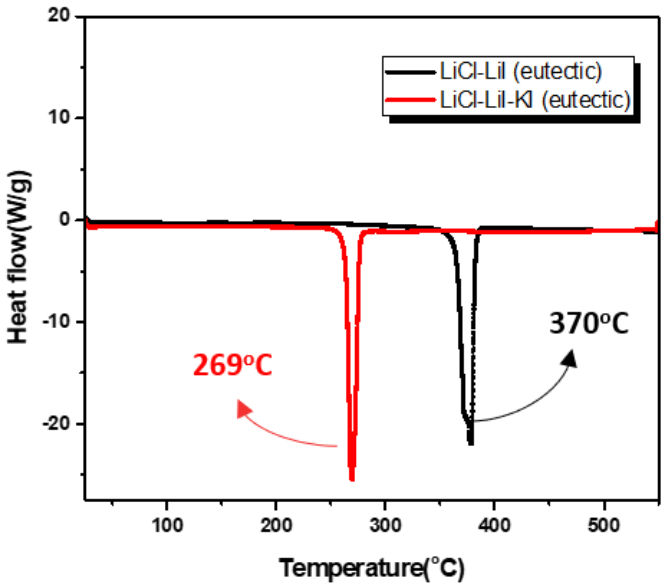

Figure 44. DSC measurement of LiCl-LiI and LiCl-LiI-KI molten salt from room temperature to 550°C

DSC measures the heat flows of sample while changing the temperature. The equipment of this experiment is Q 200 SDT (sapphire as reference) and the test condition is heating from 50°C to 550°C (10°C/min) under N_2 gas condition to prevent the contact between sample and moisture or outer atmosphere. Also, we prepared DSC sample in Ar filled glovebox to avoid contamination. As shown in figure 44, during increase temperature, at 269°C, LiCl-LiI-KI molten salt shows endothermic reaction while LiCl-LiI molten shows same reaction at 370°C. For these molten salts are solid state at room temperature so this endothermic reaction means the melting reaction to become liquid states. Through DSC data, the melting temperature of LiCl-LiI-KI molten salt is less than LiCl-LiI molten salt almost 100°C. Therefore, this tests shows the possibility of low operating temperature of liquid metal battery using LiCl-LiI-KI.

3.2.2 Density of LiCl-LiI-KI molten salt

The density of molten salts is also important to operate liquid metal battery, to separate each component. However, it is very difficult to measure the density at high temperature (~500°C). Therefore, we measured the density of molten salt at room temperature with micromeritics, AccuPyc 2 1340, Gas Pycnometer and at high temperature, using quartz crucible.

According to previous studies which measure the density of molten salt, the calculated density value was given as equation (1) with the assumption that no volume effect occurred.[26]

$$\rho = \left(\sum_i \frac{X_i}{\rho_i} \right)^{-1} \quad (1)$$

Where X_i and ρ_i represent the molar fraction and the density of constituent I in the mixture, respectively. Using equation (1), the calculated density of LiCl-LiI-KI molten salt is 3.552g/cm^3.

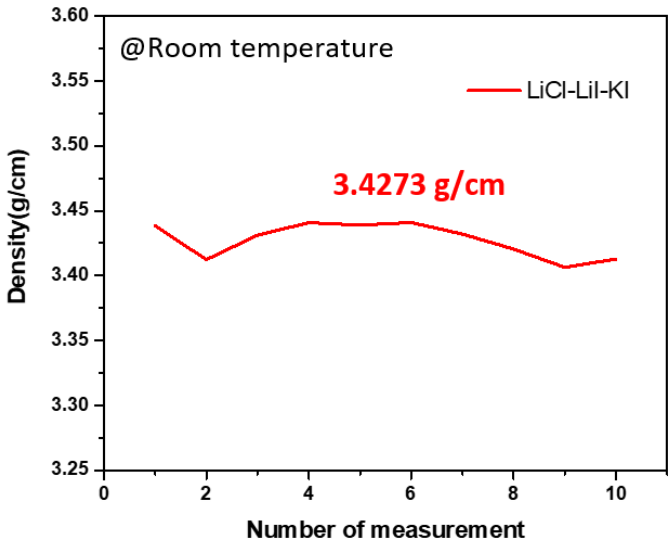

Figure 45. Density measurement of LiCl-LiI-KI molten salt using micromeritics, AccuPyc 2 1340, at room temperature

As shown in figure 45, the measured density of LiCl-LiI-KI molten salt is 3.4273 g/cm^3. This value is similar with the calculated value, so we can verify this LiCl-LiI-KI molten salt is well synthesized. Also, the 3.4273 g/cm^3 value is validated as electrolytes for Li|LiCl-LiI-KI|Bi composition because the density of Li metal is 0.534 g/cm^3 and the density of Bi metal is 9.78 g/cm^3.

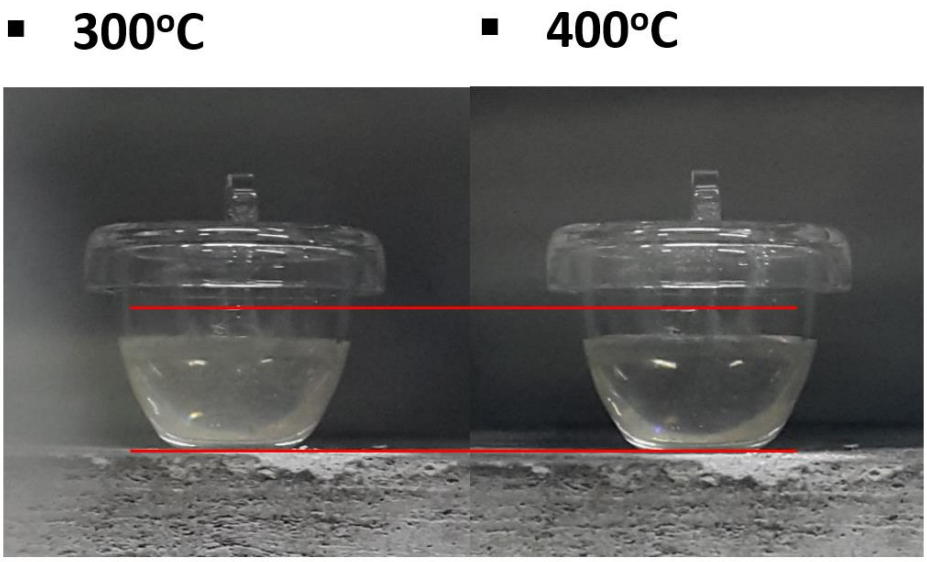

Figure 46. Density measurement of LiCl-LiI-KI molten salt over melting temperature using quartz crucible in Ar filled glovebox

As shown in figure 46, the density of LiCl-LiI-KI molten salt also measured at high temperature, 300°C and 400°C. We carved scale of volume at the quartz crucible and using them to measure the volume of molten salts. As we measure the weight of molten salt by balance and measure volume by quartz crucible at various temperature in Ar filled glovebox using mini-furnace. However, these carved scales cannot distinguish the small difference of volume change at different temperature 300°C and 400°C. The measure density of LiCl-LiI-KI molten salt at melting temperature is about 3.00 g/cm^3.

In literature, the density of liquid LiCl-LiI-KI molten salt was given as equation (2) in temperature range of 274°C ~ 437°C,

$$\rho = 3.214 - 7.850 \times 10^{-4} t \qquad (2)$$

where t is celsius temperature.[26]

According to equation (2) the calculated density of LiCl-LiI-KI molten salt is 2.76 g/cm^3 (at 300°C) and 2.69 g/cm^3 (at 400°C).

These values show a little bit difference between measured value, however, the measured value is proper to operate Li|LiCl-LiI-Ki|Bi composition according to the density of Li and Bi is 0.5049 and 10.05 g/cm^3 respectively at high temperature (~ 300°C).

3.2.3 Metal solubility of LiCl-LiI-KI molten salt

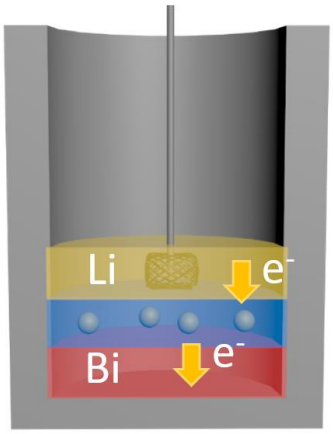

Figure 47. Scheme of electron transport in liquid metal battery by dissolved metal in electrolyte

The solubility of metal in molten salt electrolytes is important property for liquid metal battery systems, because it can cause high self-discharge current and low coulombic efficiency.[15] As shown in figure 47, through dissolved metal in electrolyte, electrons transport occur which means self-discharge in battery system. There is no definite principle for this phenomenon, several mechanisms have been proposed. These include (1) the solvation of atoms that retain their individuality and are evenly distributed throughout the volume of the solution [e.g., Na(l) = Na(in NaCl)], (2) a chemical reaction between the electrolyte and the metal through the formation of ions or subions of lower valency such as Na_2^+ or Ca_2^+ [e.g., Na(l) + Na^+ (in NaCl) = Na_2^+(in NaCl)], and (3) ionization of the metal (e.g., Na = $Na^{\bullet}$ + e`) combined with the formation of ionic vacancies (e.g., $V_{NaCl}$ = $V`_{Na}$ + $V^{\bullet}_{Cl}$) to create localized solvated electrons in anion vacancies (e.g., V_{NaCl} + Na = $Na^{\times}_{Na}$ + $e^{\times}_{Cl}$) analogous to F-center defects in ionic crystals.[15]

The method to measure the solubility of molten salt electrolyte is measuring leakage current by step-potential method.[17] As shown in figure 47, the step-potential method measured the current while apply higher voltage over than fully charged open circuit voltage. According to higher voltage over than OCV, the current flows until full charged state. In figure 48, after 8 hours, the current decrease to nearly 0 mA. This is because the cell became full-charged state by the currents and could not charge anymore. In that case, higher the applied voltage and then check the small amount of current which flows nearly 1.0 mA/cm^2 in the figure. We called this current as leakage current which flows itself at full-charged state.

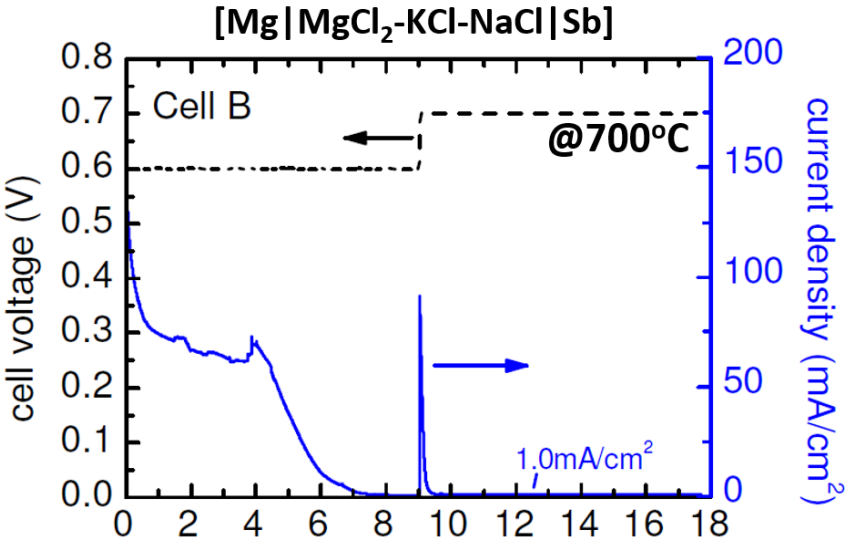

Figure 48. Step potential measurements of Mg||Sb liquid metal battery at 700°C

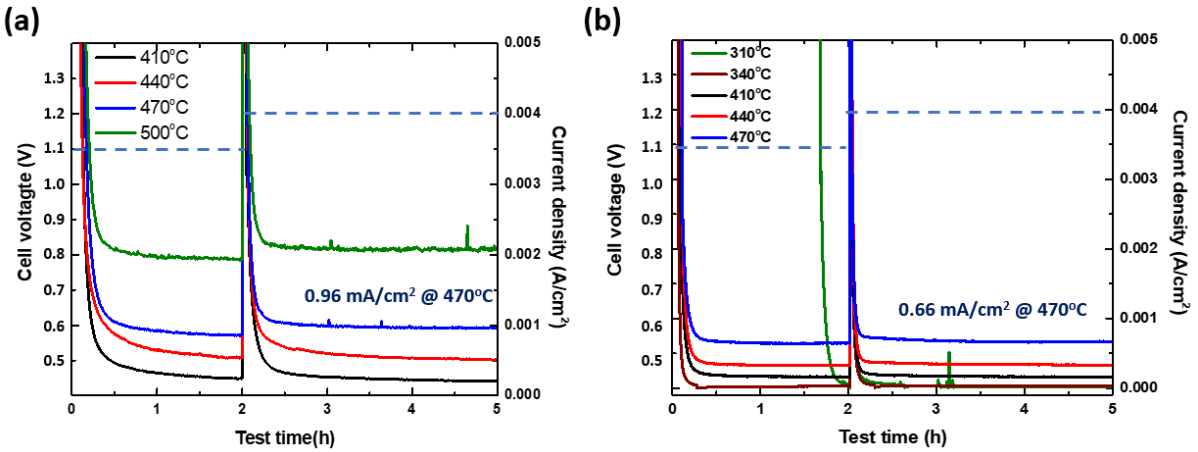

Figure 49. Step-potential method of (a) Li|LiCl-LiI|Bi composition and (b) Li|LiCl-LiI-KI|Bi composition at various temperature

As shown in figure 49, we also measured the step-potential method with Li|LiCl-LiI|Bi and Li|LiCl-LiI-KI|Bi composition. Because the open circuit voltage of Li||Bi liquid metal battery cell is nearly 0.86-0.77[27] so that we applied 1.1 V to the cell at first region and 1.2 V at second region. As shown in figure 49(a), LiCl-LiI cell shows 0.96mA/cm^2 of leakage current at 470°C. However, LiCl-LiI-KI cell shows lower leakage current, 0.66mA/cm^2 compared with LiCl-LiI cell. This is because of adding potassium ion into the Li based halide molten salt (LiCl-LiI). In literature, using multi-cation in molten salt can reduce the solubility of metal in molten salt depending on the ionic size of the foreign cation species.[28,29] There's also trends of leakage current depending on temperature. While decrease the operating temperature, each leakage

current is decreased because when temperature decrease, the solubility of metal in molten salt also decrease.[30] Therefore, through these measurement, LiCl-LiI-KI molten salts has advantage of low operating temperature and low solubility which can cause self-discharge of cell system compared with LiCl-LiI molten salt electrolyte.

3.2.4 No irreversible side reactions of spectator ions within the operating voltage window

Because molten salts are also electrolytes in liquid metal battery system, it should have no irreversible side reactions of spectator ions within the operating voltage window. We could know this operating window by the thermal decomposition voltage in molten salt.

The decomposition potential of a single molten salt can be determined theoretically from the change of the Gibbs energy of the primary cell during the electrochemical process as shown in equation (3).[31]

$$V_d = -\frac{\Delta G}{nF} \qquad (3)$$

Where V_d is the decomposition potential, ΔG is the change of free energy, and n is the valence potential. According to equation (3) and JANAF Thermochemical Tables, we could calculate the theoretical decomposition of each single molten salt electrolyte.[32]

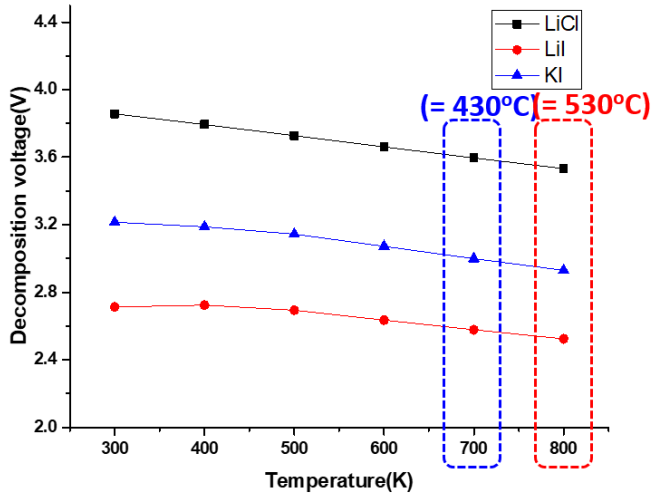

Figure 50. Theoretical decomposition voltage of single molten salt (LiCl, LiI, KI) by calculated from Gibbs free energy

Figure 50 shows the calculated decomposition voltage of LiCl, LiI, KI single molten salts. While compare with calculated values with measured values of other molten salt electrolytes, the criteria of the potential are standard hydrogen electrode. Also, there was trends in figure 50, as temperature increase, the decomposition voltage decrease.

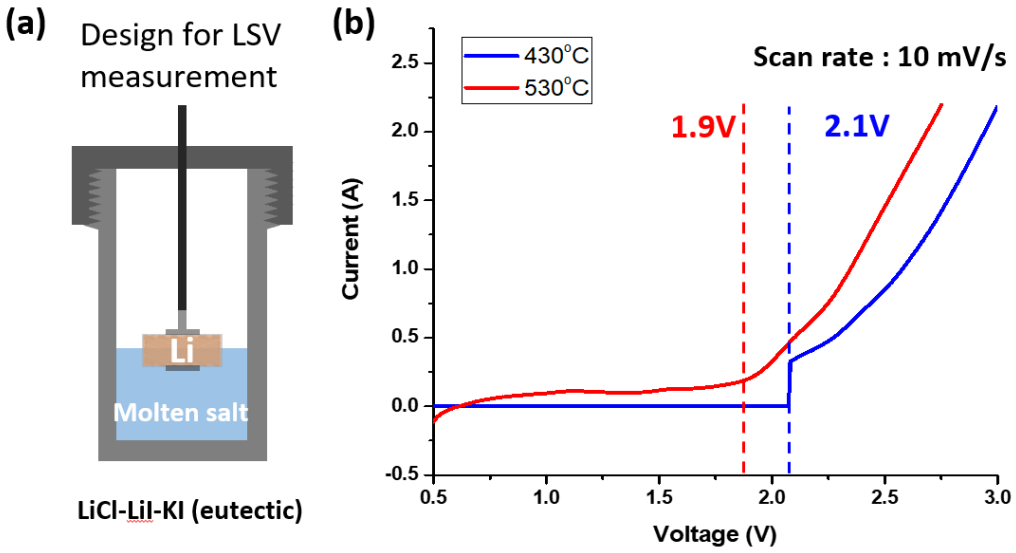

Figure 51. (a) Linear Sweep Voltammetry (LSV) measurement cell design and (b) LSV result for the tested cell at different temperature

The electrochemical window for LiCl-LiI-KI molten salt electrolyte is measured by Linear Sweep Voltammetry (LSV) by Wonatech WBCS 3000, the scan rate is 10mV/s and the voltage range is 0.5 ~ 3.0 V. The tested cell was designed as similar as LMB full cell, however, remove the cathode part, and the reference electrode and counter electrode is lithium metal anode. In figure 51(b), the decomposition of voltage of LiCl-LiI-KI molten salt appeared at nearly 2.0V ver. Li metal. Because measured data is ternary molten salt and the calculated data is single molten salt, it is difficult to compare these two graphs however, the temperature dependent trends are similar. The temperature decreases, the decomposition voltage also decreases.

3.2.5 Ionic conductivity of LiCl-LiI-KI molten salt

The ionic conductivity properties of electrolytes are very important for high rate capability and energy efficiency of liquid metal battery system. However, as same case of density measurement, it is very difficult to measure the ionic conductivity precisely at high temperature.

In literature, apparatus in figure 52(a) is used for ionic conductivity measurement, [33] however, it takes time and cost for the construct that apparatus, similar design with LMB full cell is used for measuring ionic conductivity of molten salt electrolyte in our group as shown in figure 52(b).

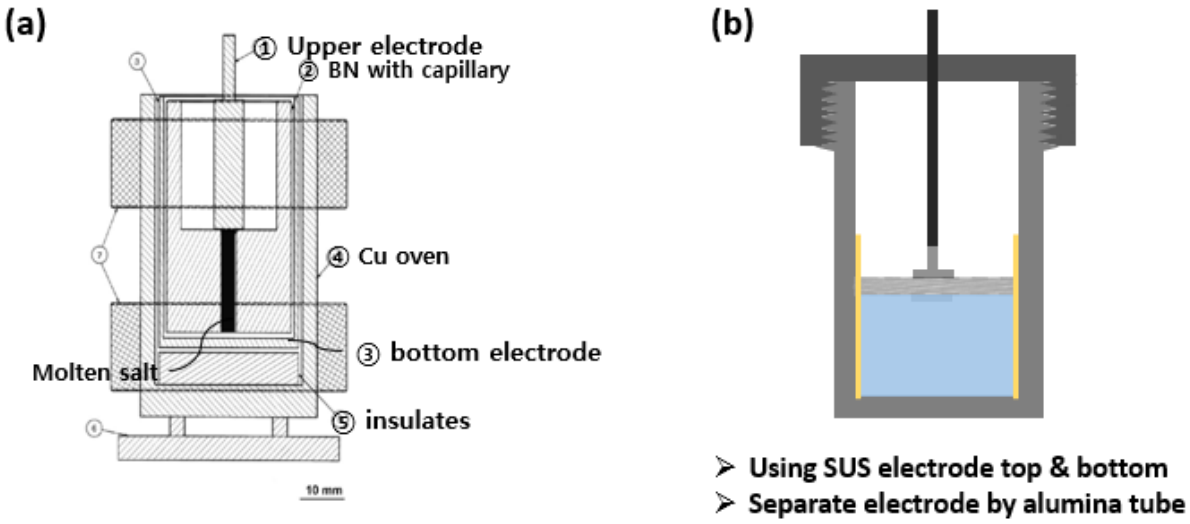

Figure 52. (a) Apparatus used for ionic conductivity measurements situated in a glove box in literature (b) apparatus for ionic conductivity measurement in our laboratory

The apparatus used in our laboratory consists of two SUS electrode which has the same area at top and bottom of the cell and the middle SUS container is separated from electrodes by alumina ceramic tube. Also, it is difficult to control the area of upper SUS electrode and the area of ceramic tube exactly, there was a small gap between them which permits flow of molten salt electrolyte and we expect this small difference can cause the error of the final measurements. The ionic measurements are tested by Electrochemical Impedance Spectroscopy (EIS) by ZIVE SP2, Wonatech in a frequency of 10^4 to 100 Hz with amplitude of 10mV.

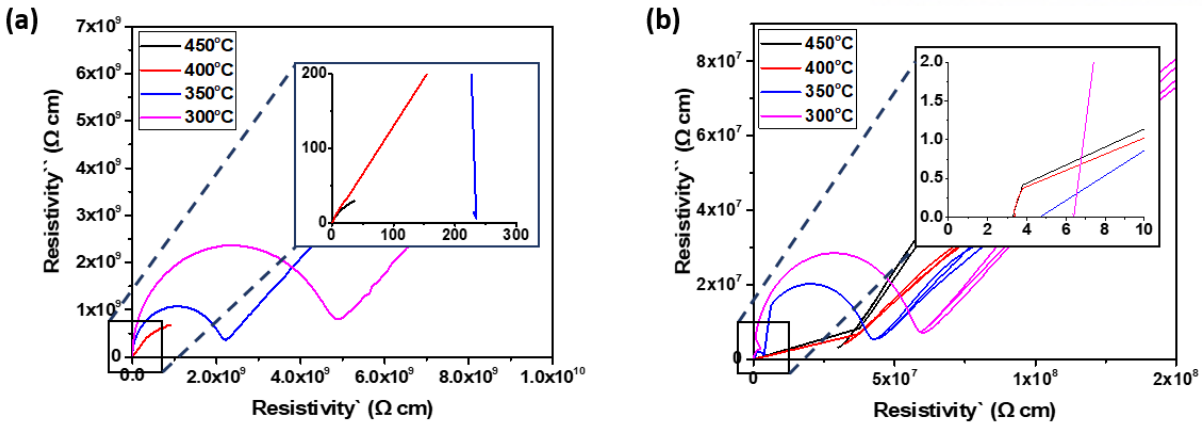

Figure 53. (a) EIS data of LiCl-LiI molten salt with magnifying the region of internal resistance, and (b) EIS data of LiCl-LiI-KI molten salt

As shown in figure 53, compare with the LiCl-LiI and LiCl-LiI-KI molten salt, the internal resistance shows different trends during decreasing temperature. In case of LiCl-LiI molten, when temperature decrease under 350°C, which is lower than the melting temperature (370°C), the internal resistance increases over 200Ω. The reason for this is because at the solid state of LiCl-LiI molten salt, the salt cannot transport the ions as fast as liquid state. However, in LiCl-LiI-KI molten salt, because the melting point is lower than LiCl-LiI (265°C), it shows similar resistance near 10Ω when temperature goes under 300°C. According to this ionic conductivity results, we found the possibility of low operating temperature liquid metal battery using LiCl-LiI-KI molten salt as electrolyte.

3.3 Full cell performance with Li|LiCl-LiI-KI|Bi composition

In the previous chapter, the intrinsic properties of LiCl-LiI-KI molten salt have been measured as electrolyte for liquid metal battery system. According to the DSC and EIS data, the properties of low melting temperature and maintained ionic conductivity at the temperature are verified. Therefore, we tried to make full cell system using LiCl-LiI-KI molten salt with lithium metal anode and bismuth metal cathode here.

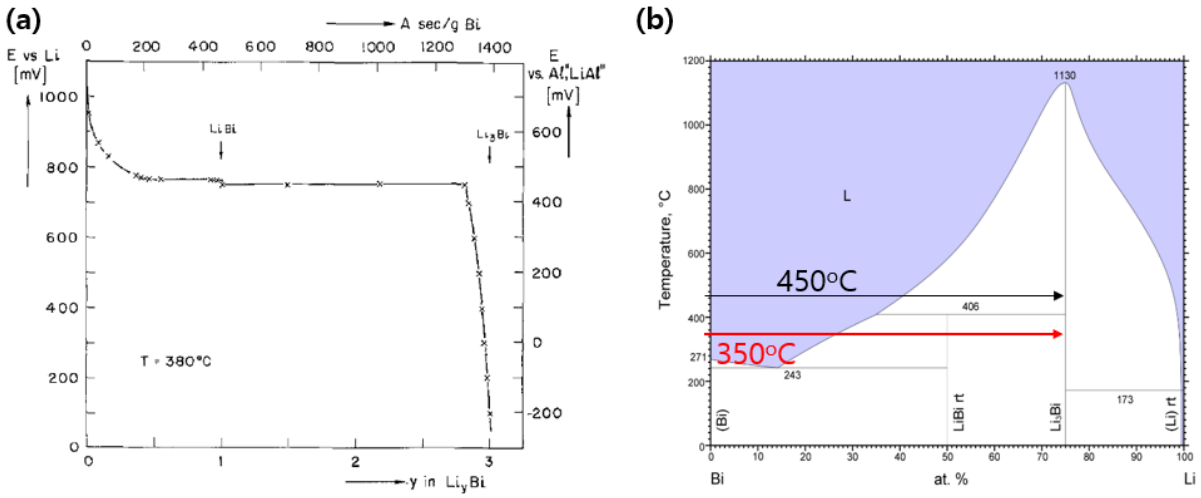

Figure 54. (a) The coulometric titration curve for the system Li-Bi at 380°C and (b) the phase diagram of Li-Bi alloy system

Before operating the cell, we could expect the voltage profile of the Li-Bi system by coulometric titration data in figure 54(a) at 380°C. In literature, the curve of the Li-Bi system is interpreted as a large range of solubility of lithium in bismuth is followed by the two-phase region of Bi in equilibrium with LiBi. The second plateau indicates the coexistence of LiBi with Li_3Bi region.[27] According to the phase diagram in figure 54(b), during Li dissolves in Bi metal alloy to form Li-Bi alloy, while over 405°C, only Li_3Bi phase are formed, under 405°C two phases are formed, LiBi and Li_3Bi. Therefore, as shown in figure 54(a), there were two voltage plateau one for liquid + LiBi region and one for LiBi + Li_3Bi region.

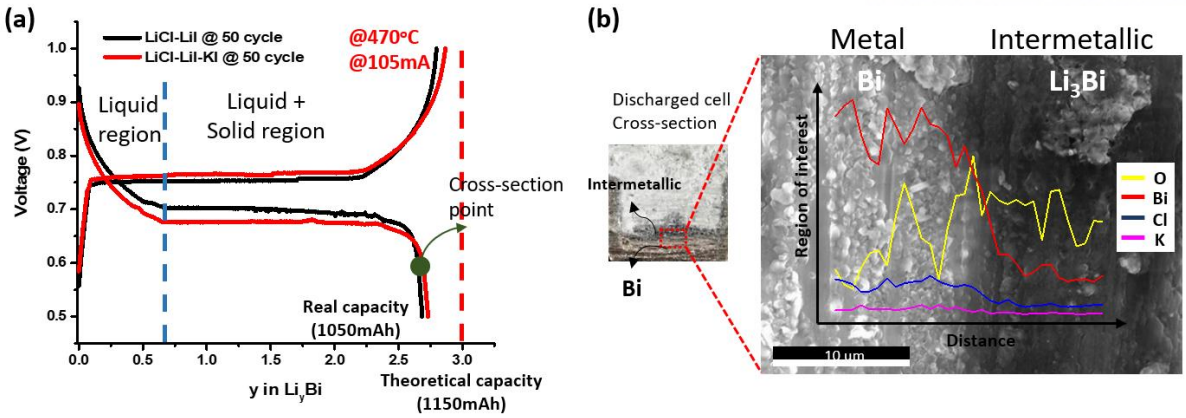

Figure 55. (a) Voltage profile of Li|LiCl-LiI|Bi and Li|LiCl-LiI-KI|Bi liquid metal batteries and (b) SEM EDS data of cross-section image at full discharged state

Figure 55(a) shows the voltage profile of Li|LiCl-LiI|Bi cell and Li|LiCl-LiI-KI|Bi cell at 470°C with 105mA, 50mA/cm^2 current density. According to the Li-Bi phase diagram in figure 59, at 470°C, no LiBi phase are formed, just Li_3Bi solid phase are formed during charging and discharging so, only one plateau occurred in both cells. Although change the electrolyte to LiCl-LiI-KI molten salt, there was no capacity difference and same plateau point which occur at state change form liquid to solid. The same plateau point at same temperature means that the electrolytes transport the same amount of Li to Bi alloy. Also, compare with the theoretical capacity which means 75% of mole fraction of Li metal in Bi metal,[22] in this cell 1150mAh according to the amount of Bi cathode, they show a little bit less charge and discharge capacity. According to these two points, we could verify the role of the LiCl-LiI-KI molten salt electrolyte did the same role as LiCl-LiI molten salt at 470°C. Although the voltage gap is of the full cell is a little bit larger at LiCl-LiI-KI because of low ionic conductivity, it doesn't show any difference with plateau point and capacity. The role of LiCl-LiI-KI molten salts are also verified by cross-section SEM EDS (Scanning Electron Microscope Energy Dispersive Spectrometer) analysis. At full discharged state, we made cross-section cell by cutting cell by half and got the image in figure 55(b). There were to regions at the bottom of the cell, bismuth metal region and Li_xBi intermetallic region. According to the figure 55(a), graph, all the metallic parts should be changed to Li_xBi phase, however, the cell used in figure 55(b) is not the cathode limited cell, but anode limited cell so it shows many regions of bismuth metallic part. According to figure 55(b), the interface of the two region is analyzed by SEM EDS. Although the element of lithium cannot be detected directly by EDS, trace Li elements indirectly by detecting oxygen in intermetallic compound. This is because lithium easily oxidized during sample preparation process.[35] At the interface of the metal and intermetallic compound, the intensity of bismuth element changed sharply. In the right part, the intensity of bismuth element is less than oxygen, so that it means

that this phase is Li_3Bi phase and the left part means bismuth phase where Li dissolves a little. However, in both case there was little intensity of potassium and no intensity difference at these two phases. These phenomena mean that potassium doesn't participate the redox reaction during charging and discharging process. Therefore, the function of potassium ion in molten salt is reducing the melting temperature without redox reaction while decreasing a little bit of ionic conductivity.

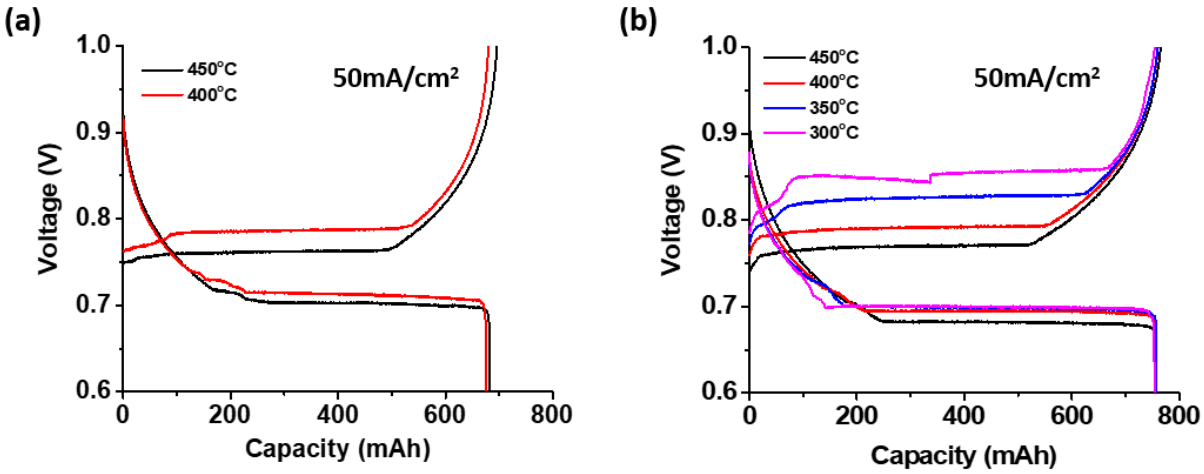

Figure 56. Voltage profile of Li|LiCl-LiI|Bi cell (a) and Li|LiCl-LiI-KI|Bi cell (b) during decrease the operating temperature

After comparing the voltage profile at 470°C, both cells tested at various temperature while decrease the operating temperature per 50°C as shown in figure 56. Although, the cell using LiCl-LiI molten salt electrolyte couldn't operate under 400°C, LiCl-LiI-KI cell can operate at 300°C. Under the temperature both cells show the high overpotential near 10V due to high internal resistance of solid state. Compare with Li|LiCl-LiI|Bi cell, LiCl-LiI-KI cell shows lower operating temperature at 300°C. The unusual point of this voltage profile is while decrease the operating temperature, the cell shows larger voltage gap but maintained discharge plateau. Because of decreased ionic conductivity, the larger voltage gap was expected, but the discharge plateau didn't decrease. In literature, the reason of this is because of Li solubility of Bi.

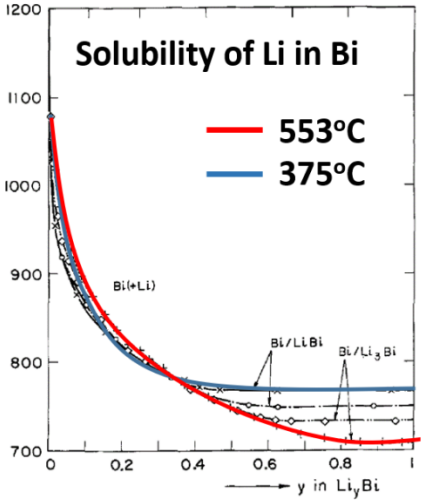

Figure 57. The solubility of lithium in bismuth at different temperatures. The steady-state galvanic cell voltage vs. lithium is plotted as a function of the amount of lithium electrochemically titrated into liquid bismuth[27]

As shown in figure 57, the start point of voltage plateau in Li-Bi alloy depends on temperature. At lower temperature, the voltage plateau starts earlier than high temperature. This because at high temperature, much more Li can dissolve in Bi in liquid state. At low temperature, the amount of liquid Li-Bi alloy is decreased, so the plateau which means the mixed region of liquid + solid appeared earlier. As a result, at low temperature the voltage plateau increases as shown in figure 56 and figure 57.

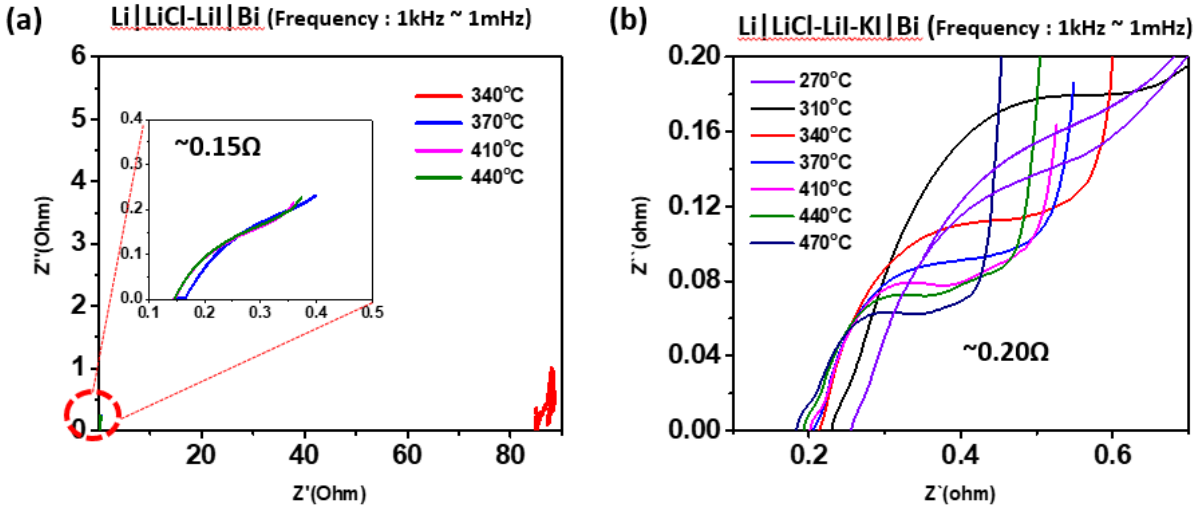

Figure 58. Full cell EIS of Li|LiCl-LiI|Bi cell (a) and Li|LiCl-LiI-KI|Bi cell

Figure 58 shows the EIS data of LMB full cell at different molten salt electrolytes. Using LiCl-LiI molten salt electrolyte, when the temperature is decreased under 370°C, the internal resistance increases sharply over 80 ohms. However, in LiCl-LiI-KI cell shows similar internal resistance while decrease the temperature under 270°C. According to these two data, voltage profile graph of figure 61 can be explained why LiCl-LiI-KI shows lower operating temperature.

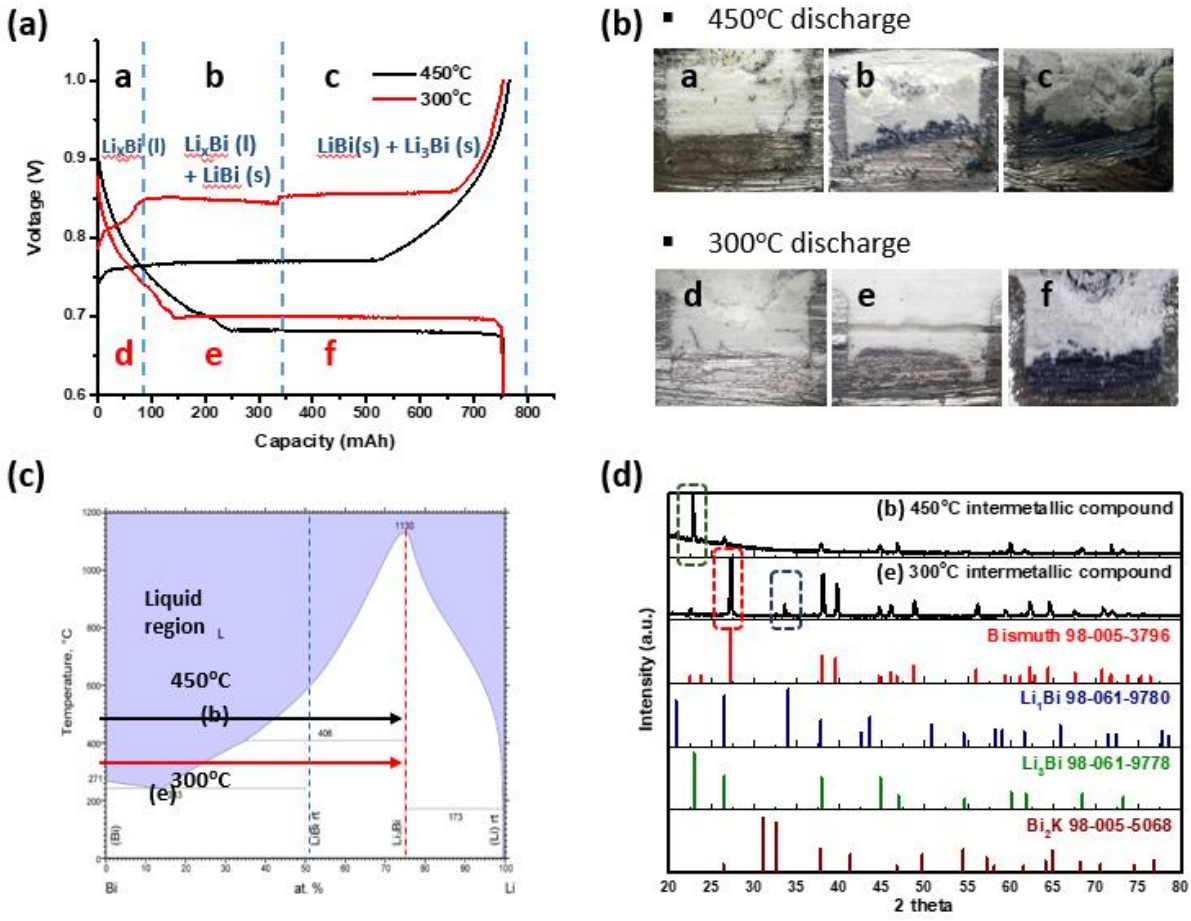

Figure 59. (a) Comparison of voltage profile, (b) phase formation of Li-Bi at different temperature and (c) phase diagram at each temperature and (d) XRD analysis of the phases

Figure 59(a) shows the voltage profile comparison between operating at 450°C and 300°C which appeared at figure 56(b). Because according to phase diagram in figure 59(c) at different temperature in criteria of 405°C, different phases are occurred during alloying Li-Bi. At 450°C, only Li_3Bi solid phase are formed, so that in figure 59(a) there is only one voltage plateau. However, at 300°C, LiBi and Li_3Bi phases are formed during alloying process so the voltage profile shows two plateau LiBi + Li3Bi region for b, and LiBi + liquid region for c during charging process. To verify the phase formation of each region, prepare the cross-section image of the cell at each region during discharge at 450°C, full charged (a), first plateau (b), full

discharge (c) and at 300°C, full charged (d), first plateau (e), full discharge (f). Compare with each state, full charged and full discharged states show similar phase formation, the bismuth metal shows color of steel and Li_3Bi phase seems a little bit navy color. However, in first plateau region (e), the color of the intermetallic compound is dark gray, which looks different with Li_3Bi phase, so we expected this region is LiBi region. Therefore, intermetallic compound of (b) and (e) regions are analyzed by XRD (X-ray Diffraction) in figure 59(d). As we expected, the intermetallic compound of region (b) shows Li_3Bi phase, however, the intermetallic compound of region (e) shows the mixture of LiBi region and bismuth region. This is because the amount of intermetallic compound of region (e) is small, so when we cut the sample from cross-sectioned cell, bismuth metal was included at the bottom of the sample. The next thing we can check here is there is no potassium bismuth intensity of these two regions. That means potassium doesn't participate the redox reaction here.

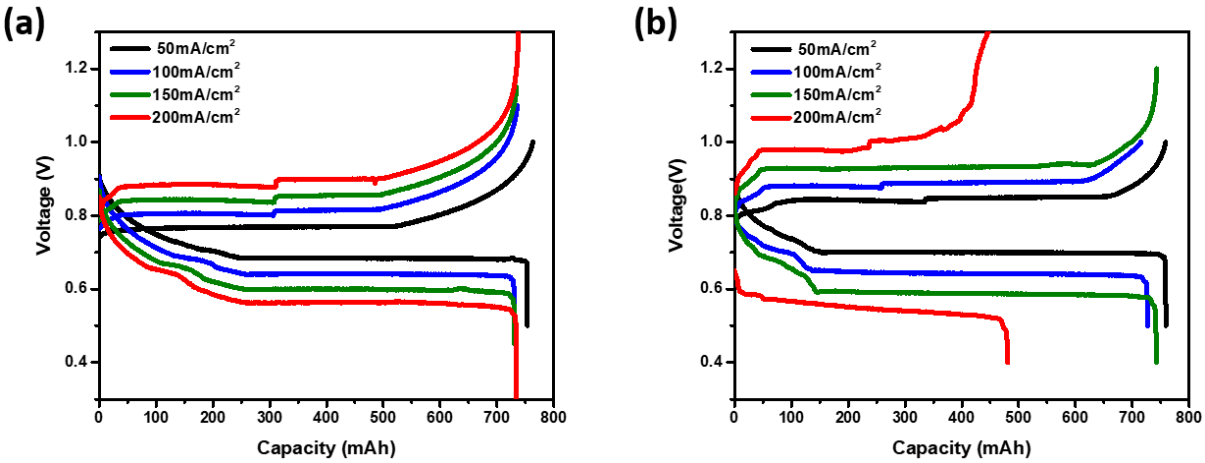

Figure 60. Rate capability test of Li|LiCl-LiI-KI|Bi cell at different temperature, 450°C (a) and 330°C (b).

According to previous tests, we could know that using LiCl-LiI-KI molten salt electrolyte we could reduce the operating temperature. Now we test the performance of each temperature by rate capability test at 450°C and 330°C. As shown in figure 60, at 450°C there is no capacity fade at 200mA/cm^2 however, at 330°C, capacity fade occurred at 200mA/cm^2. In literature, the reason for this poor rate capability can be separated as two factors. Charge transfer kinetics and Mass transport kinetics.

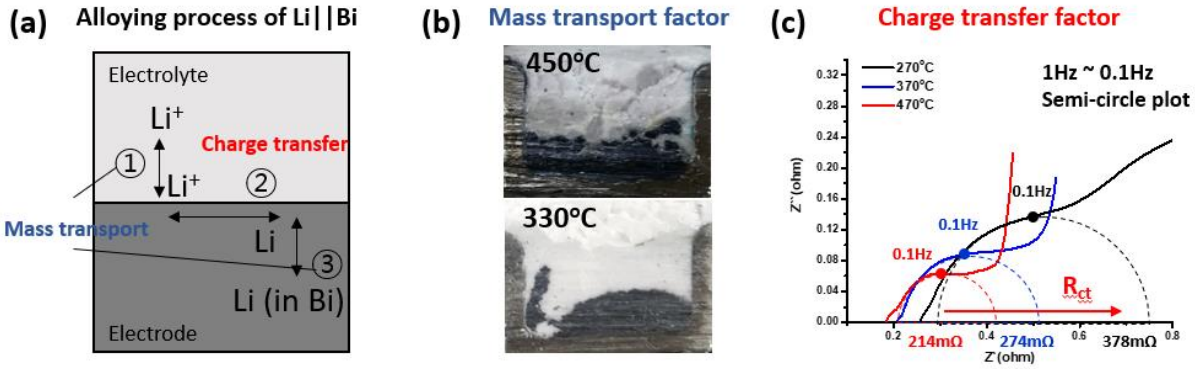

Figure 61. Kinetics in alloying process of Li-Bi alloy system (a) and full discharge at 200mA/cm^2 cross-section image (b) and Li|LiCl-LiI-KI|Bi full cell EIS semi-circle plot data (c)

The alloying process of Li||Bi liquid metal battery system can be expressed as figure 61(a).[36]
1) Mass transport process of Li cation in molten salt electrolyte to the surface of the electrode
2) Charge transfer of Li cation to Li metal in Bi alloy at the interface of electrolyte and electrode
3) Mass transport of reduced metal in bismuth electrode.

In literature, mass transport kinetics can cause the capacity fade at high current density because of the slow distribution of anode metal in cathode alloy and means inability to use all the amount of cathode.[37] To check this point, cross-section the cells which are operated with 200mA/cm^2 current at different temperatures. However, the cross-section cell images show the formation of homogeneous intermetallic compound at high current discharge. Therefore, we expect the cause of the capacity fade should be charge transfer at the interface of the electrolyte and electrode. According to figure 61(c), the semi-circle of the cell, which means charge transfer resistance increase when temperature goes down.

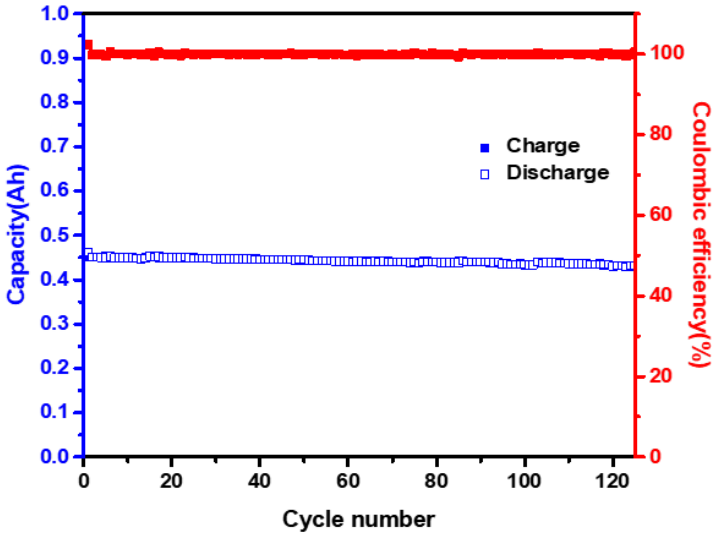

Figure 62. Cycle performance of Li|LiCl-LiI-KI|Bi cell at 330°C, 100mA/cm^2

Finally, we tested the cycle performance of the cell using LiCl-LiI-KI molten salt at 330ºC. Because of the test is ongoing, the cycle life of the cell is only 120 cycle, however it shows 99.9% of coulombic efficiency and stable cycle performance until 120 cycle.

3.4 Summary

To reduce the operating temperature of liquid metal battery system, LiCl-LiI-KI molten salts are used as electrolyte in Li||Bi composition. Before the test of LiCl-LiI-KI LMB cell, we must know the intrinsic properties of molten salts such as density, ionic conductivity and so on to fulfill the requirements of the electrolytes for liquid metal battery. According to DSC and ionic conductivity measurement of the molten salt, we found the possibility of low temperature operating. The Li|LiCl-LiI-KI|Bi full cell operates at 300ºC, the lowest operating temperature in liquid metal battery systems. While decrease the operating temperature, discharge voltage doesn't decrease at 50mA/cm^2 until 300ºC, however, it shows more capacity fade at high current. Also, the phase formation of different temperature is analyzed by cross-section image and XRD and finally the cell shows stable cycle performance during 120 cycle, 99.9% of coulombic efficiency.

4. Conclusion

Energy Storage Systems (EES)s have been received attention for its various applications such as peak shaving, integration of renewable energy and frequency regulation. Among many candidates of ESS such as LIBs, thermal batteries and NaS batteries and so on, liquid metal battery can be a proper candidate for the high power ESS because of its high current density and stable cycle life properties. However, liquid metal battery has low operating voltage and high operating temperature problems, therefore, the research trends of the liquid metal battery system is increasing the operating voltage and decrease the operating temperature. Here, in this thesis we focus on the decrease the operating temperature of LMB.

Before the test new composition or materials, we designed the cell and optimized the test condition of the cell to get constant, repeatable data. Therefore, we considered two factors which affect the cell performance, repeatability factor and unstable voltage factor. According to the factors, revise and develop the cell test condition and finally get the repeatable data which shows less voltage gap by precise active area. Also, by cross-section image after cycling, we could verify Li metal exists in Ni-Fe foam even at full-discharged state at cathode limited electrode ratio. This characteristic keeps the cell shows repeatable voltage profiles.

Because of the high temperature problems of liquid metal battery system such as thermal corrosion, we try to reduce the operating temperature of LMB system. In the previous lowest operating temperature composition, the melting temperature of electrolyte is higher than other compositions. Therefore, we tested new composition of molten salt electrolyte, LiCl-LiI-KI about its density, ionic conductivity and so on. Through the salts, we made Li|LiCl-LiI-KI|Bi composition of liquid metal battery and decrease the operating temperature at 300°C. While decreasing the operating temperature (400 ℃→300 ℃), the energy efficiency decrease (85.1% → 81.9%) because of decreased ionic conductivity of electrolyte, increased voltage gap at current density of 50 mA/cm². However, lowering temperature also increase the cell open circuit voltage because Li solubility in Bi metal in liquid state decreased. Also, we analyzed the phase formation of Li-Bi alloying process at different temperature by cross-section and XRD analysis. The rate capability test at different temperature shows the higher voltage gap and capacity fade at low temperature (300°C) and we analyzed this with EIS data of full cell at various temperature. Finally, the Li|LiCl-LiI-KI|Bi composition liquid metal battery operates over 120 cycle without capacity fade at 330°C.

5. References

[1] Reserve electric generating capacity helps keep the lights on, U.S. Energy Information Administration, 2012

[2] Power supply and demand, Korea Power Exchange, 2018

[3] Korea Electric Power Corporation, Electric rates table for general service (A)

[4] Edmund G. Brown Jr., Governor, California energy commission, New solar homes partnership market report, 2016

[5] Sang-Youp Lee, Admendment direction of 2030 greenhouse gas reduction roadmap based on national energy transition policy, 2018

[6] LG Chemistry, ESS battery division, ESS for grid application

[7] Joe Eto et al., 2010, Use of a frequency response metric to assess the planning and operating requirements for reliable integration of variable renewable generation, Lawrence Berkeley National Laboratory

[8] Oh Sang Hyun, Song Lak Kyung, An analysis of success factors of FR ESS projects in South Korea, 2017

[9] Devon Manz, Richard Piwko, Nicholas Miller, The role of energy storage in the grid, 2012, IEEE power & energy magazine, 1540-7977

[10] Ioan Sarbu, Calin Sebarchievici, A Comprehensive Review of Thermal Energy Storage, sustainability, 2018, 10, 191

[11] Ioan Sarbu, Calin Sebarchievici, Solar Heating and Cooling: Fundamentals, Experiments and Applications; Elsevier: Oxford, UK, 2016

[12] Guruprasad Alva, Yaxue Lin, Guiyin Fang, An overview of thermal energy storage systems Energy 144 (2018) 341-378

[13] Nam Hyun-woo, Frequent fire raising concerns over safety of solar energy, 2018.12.18 The Korea Times

[14] NGK INSULATORS, LTD, Why NAS, www.ngk.co.jp

[15] Liquid Metal Batteries : Past, Present, and Future, Chemical review, 2013, 113, 2075 – 2099

[16] Liquid Metal Electrodes for Energy Storage Batteries, Kangli Wnag, Kai Jiang, and Donald R. Sadoway, Advanced energy materieals, 2016, 6, 1600483

[17] Magnesium-Antimony Liquid Metal Battery for Stationary Energy Storage, David J. Bradwell, Hojong Kim, Aislinn H. C. Sirk, and Donald R. Sadoway, Journal of the American chemical society, 2012, 134, 1895 – 1897

[18] Lithium-antimony-lead liquid metal battery for gird-level energy storage, Kangli Wnag, Kai jiang, Donald R. Sadoway, Nature, vol 514, 2014

[19] Calcium-based multi-element chemistry for grid-scale electrochemical energy storage, Takanari Ouchi, Hojong Kim, Brian L. Spatocco and Donal R. Sadoway, 2016, Nature communications, doi : 10.1038

[20] Faradaically selective membrane for liquid metal displacement batteries, Huayi Yin, Brice Chung and Donald R. Sadoway, Nature energy, doi : 10.1038

[21] Low-temperature molten salt electrolytes for membrane-free sodium metal batteries, Journal of the electrochemical society, 162 (14) A2729-A2736 (2015)

[22] Self-healing Li-Bi liquid metal battery for grid-scale energy storage, Journal of Power Sources 275 (2015) 370-376

[23] LiCl-LiI molten salt electrolyte with bismuth-lead positive electrode for liquid metal battery, Journal of Power Sources, 2018, 377, 87 – 92

[24] Thermal activated (thermal) battery technology part 2. Molten salt electrolytes, Patrick Masset, Ronald A. Guidotti, Journal of Power Sources, 164 (2007) 397-414

[25] Iodide-based electrolytes : A promising alternative for thermal batteires, Partrick masset, Journal of Power Sources 160 (2006) 688-697

[26] Density and electrical conductivity of molten LiI-LiCl-KI eutectic, N.P. Yao, ECS, 1972

[27] Thermodynamic properties of the intermetallic systems lithium-antimony and lithium-bismuth, W. Weppenr and R.A. Huggins, J. Electrochem. Soc. 1978, 125, 7

[28] E.A. Ukshe, N.G. Bukun, Russ. The dissolution of metals in fused halide, Chem. Rev. 30 (1961) 90 – 107

[29] Hojong Kim, Dane A. Boysen, Takanari Ouchi, Donald R. Sadoway, Calcium-bismuth electrodes for large-scale energy storage (liquid metal batteries), Journal of Power Sources, 241 (2013) 239-248

[30] Mixtures of metals with molten salts, M.A. Bredig, 1963, ORNL-3391, UC-4-Chemistry, TID-4500 (20th ed., Rev.)

[31] Ruren Xu, Qiang Su, Cahpter 2 – High-temperature Sysnthesis, Morern Inorganic Synthetic Chemistry, 2011, 9-38

[32] D. R. Stull and H. Prophet, JANAF Thermochemical Tables SECOND EDITION, 1971

[33] Patrick masset, Antoine Henry, Jean_Yves Poinso, Jean-Claude Poignet, Ionic conductivity measurements of molten iodide-based electrolytes, 2006, Journal of Power Sources, 160, 752-757

[34] Gasior W., Moser Z., and Zakulski W., Bi-Li system. Thermodynamic properties and the phase diagram calculations, 1994, Arch. Metall., Vol. 39, 355-369

[35] Hamiao Li, Kangli Wang, Shijie Cheng, and Kia Jiang, High Performance Liquid metal Battery with Environmentally Friendly Antimony-Tin Positive Electrode, ACS Applied Material & Interfaces, 2016, 8, 12830-12835

[36] Jocelyn M. Newhouse and Donald R. Sadoway, Charge-Transfer Kinetics of Alloying in Mg-Sb and Li-Bi Liquid Metal Electrodes, Journal of The Electrochemical Society, 2017, 164 (12) A2665-A2669

[37] Takanari Ouchi, Hojong Kim, Xiaohui Ning, and Donald R. Sadoway, Calcium-Antimony Alloys as Electrodes for Liquid Metal Batteries, Journal of The Electrochemical Society, 161 (12) A1898-A1904 (2014)

6. Acknowledgements

석사 학위를 받기까지 2년 동안의 연구실 생활은 저의 인생에 있어서 정말 뜻 깊은 시간이었습니다. 처음 지원하였었던 대학원이 떨어지고 다시 준비하고 들어올 때까지 많은 사람들의 도움을 받아 준비하였고, 힘들게 들어온 만큼 더 열심히 보람차게 석사 기간을 보내야겠다고 다짐했던 게 엊그제 같은데 벌써 졸업을 앞두고 있다니 아쉬운 마음이 듭니다. 먼저 부족한 저를 지도해 주시고 제가 지속적으로 연구할 수 있는 기회를 주신 김영식 교수님께 진심으로 감사의 말씀을 전하고 싶습니다. 교수님께서 주신 기회가 아니었다면 아마 연구와는 인연이 없는 다른 삶을 살았을 것이라고 생각합니다. 항상 건강하시고 잘 지내셨으면 좋겠습니다. 2년동안 힘들고 기쁜 일을 함께 했던 저희 실험실, YK group 멤버들에게도 감사의 말을 전하고 싶습니다. 연구에 대한 자세와 학위의 의미에 대해 생각해 볼 수 있게 도와 주신 황수민 박사님, 인도 노래도 알려주시고 항상 친절하게 대해주시는 Kumar 박사님, 항상 웃으며 인사해 주시는 Kishor 박사님에게도 감사드립니다. 특히 처음 연구실을 들어왔을 때부터 지금까지 많이 도와주신 랩장 현태형, 액체금속전지에 대해 알려주신 준수형에게도 정말 감사드립니다. 석사 졸업을 준비할 때뿐만 아니라 평소에도 엄청 도와주시는 영진이형, 실험실의 전반적인 부분을 관리해 주시느라 고생하신 진협이형, LMB 관련 논문이 있으면 알려주시는 용일이형, 항상 재미있고 활기찬 기운으로 랩에 활력을 불어넣어주시는 현우형, 같이 놀구 장난치고 존재만으로 매력적이신 진호리형까지 모든 분들께 정말 감사하다고 전해드리고 싶습니다. 최근 운동도 같이 하구 성격 매너 모두 좋으시지만 늘 행복을 찾으시는 영준이형, 옆에서 이상한 장난을 치며 힘들 때 마다 기운을 주시는 정선이형, 비슷한 취미를 가져서 공감대를 형성할 수 있는 우석이형, 이번에 같이 졸업 준비하며 취업하신다고 고생하신 혜인이 누나, 같이 입학할 때부터 친구처럼 잘 놀아주신 천사같은 다송이 누나, 매일매일 멸치라고 놀리면서 운동의 동기부여를 만들어 주는 제희, 친구처럼 편하게 대해주시고 듬직한 느낌을 주시는 남혁이형, 계속 영어로 얘기하여 영어회화가 늘 수 있게 도와준 Fahmi 까지 연구실 사람들이 있어 2년 동안 행복하게 지낼 수 있었습니다.
대학원 기간 동안 저를 믿고 거리낌없이 지원해 주신 아버지, 항상 저를 위해 기도해 주시는 어머니, 취직해서 고생하고 있지만 항상 친구같이 편안하게 대해주는 우리 형에게도 항상 고맙고 사랑한다고 전하고 싶습니다. 학부때부터 같이 오랜 시간을 보내왔지만 지금도 같이 잘 놀아주는 내 친구 재호에게도 고맙고, 마지막으로 지치고 힘들 때나 기쁜 순간마다 항상 옆에 있어준 밥 잘 먹어주는 여자친구 혜지에게도 너무너무 감사하다고 말해주고 싶습니다.

위에 다 적지는 못하였지만 정말 많은 사람들의 도움으로 여기까지 올 수 있었고, 지금의 저를 성장하게 만들어 주셨다고 생각합니다. 앞으로도 더 열심히 살며 성장하여 제가 받았던 도움을 다시 돌려드릴 수 있도록 노력하며 살아보도록 하겠습니다.
다시 한번 저를 도와 주신 모든 분들께 감사의 인사를 전합니다.